Power Flow Analysis of Islanded Microgrids: A Differential Evolution Approach

ABHISHEK KUMAR[ID],[1] **BABLESH KUMAR JHA**[2], **SWAGATAM DAS**[3], **AND RAMMOHAN MALLIPEDDI**[ID],[4], (Senior Member, IEEE)

[1]Department of Electrical Engineering, Indian Institute of Technology (BHU), Varanasi 221005, India
[2]Department of Electrical Engineering, Indian Institute of Technology Gandhinagar, Gandhinagar 382355, India
[3]Electronics and Communication Sciences Unit, Indian Statistical Institute, Kolkata 700108, India
[4]Department of Artificial Intelligence, School of Electronics Engineering, Kyungpook National University, Daegu 702701, South Korea

Corresponding author: Rammohan Mallipeddi (mallipeddi.ram@gmail.com)

ABSTRACT Power flow (PF) analysis of microgrids (MGs) has been gaining a lot of attention due to the evolution of islanded MGs. To calculate islanded MGs' PF solution, a globally convergent technique is proposed using Differential Evolution (DE)- a popular optimization algorithm for global non-convex optimization. This paper formulates the PF problem as a constrained optimization problem (COP) considering all the operating conditions of the Droop Controlled Islanded MGs (DCIMGs). To solve the proposed COP, ϵDE-NGM, (Epsilon based Differential Evolution with Newton-Gauss-based mutation) is proposed. The proposed algorithm, ϵDE-NGM, is a novel variant of DE since it comprises a novel mutation operator, Newton-Gauss-based mutation (NGM). NGM includes all the important features of DE's mutation strategies as well as reduces the constraint violation by utilizing the information of constraint-space. Numerical experiments validate that the global convergence ability of proposed algorithms in solving COPs than existing state-of-the-art algorithms. Furthermore, the proposed algorithm as a PF tool has better robustness than existing tools on ill- and well-conditioned systems with heavy loads, different limit violations, and inappropriate final solutions (far from the flat start). The performed comparative analysis confirms good agreement of accuracy and efficacy with the existing method for islanded MG's PF.

INDEX TERMS Constrained optimization problem, differential evolution, islanded microgrid, power flow, distributed generation.

NOMENCLATURE

α	Active power exponent
$\bar{x}_L$	Lower bound of search space
$\bar{x}_U$	Upper bound of search space
$\bar{x}_\theta$	Top $\theta-$th individuals
β	Reactive power exponent
$\Delta \bar{x}$	Increment expected in point $\bar{x}$
$\Delta C(\bar{x})$	Constraint violation vector
ω	Operating system frequency
ω_0	Nominal frequency of the system
$\phi(\bar{x})$	Degree of the constraint violation
B_{ij}	Susceptance of line between i^{th} and j^{th} bus
$C(\bar{x})$	Constraints vector
C_p	Frequency dependability coefficient for active power

C_q	Frequency dependability coefficient for reactive power
cp	Control parameter for reduction speed of the $\epsilon-$level
CR	Crossover rate
D	Dimension of the problem
F	Scaling factor parameter
$f(\bar{x})$	Objective function
G_{ij}	Conductance of line between i^{th} and j^{th} bus
g_i	i^{th} inequality constraint
h_j	j^{th} equality constraint
mp_i	Reactive power static droop gain
$Nbus$	Total number of buses
ng	Number of inequality constraints
nh	Number of equality constraints
np_i	Active power static droop gain
$P_{0,l,k}$	Nominal active power load demand at k^{th} bus

$P_{i,dg}$	Active power injection by DG at i^{th} bus
P_i	Active power injection at i^{th} bus
$P_{j,max}$	Maximum active power limit of DG at j^{th} bus
$P_{j,min}$	Minimum active power limit of DG at j^{th} bus
$P_{l,k}$	Active power load demand at k^{th} bus
$Q_{0,l,k}$	Nominal reactive power load demand at k^{th} bus
$Q_{i,dg}$	Reactive power injection by DG at i^{th} bus
Q_i	Reactive power injection at i^{th} bus
$Q_{j,max}$	Maximum reactive power limit of DG at j^{th} bus
$Q_{j,min}$	Minimum reactive power limit of DG at j^{th} bus
$Q_{l,k}$	Reactive power load demand at k^{th} bus
r	Resistance of line
S_{dg}	Set of droop buses
V_k	Voltage at k^{th} bus
$V_{m,k}$	Imaginary part of voltage at k^{th} bus
$V_{r,k}$	Real part of voltage at k^{th} bus
x	Reactance of line
z	impedance of line

I. INTRODUCTION

A microgrid (MG) has been recognized as a collection of Distributed generation units (DGs) interconnected with thermal and electrical loads, energy storage units, and capacitor banks. Besides, it functions as a single small scale distribution system. By using power electronic controls and interfaces, MG's reliability, security, and controls can be enhanced [1], [2]. An MG can run in an islanded or grid-connected mode. In an islanded mode, DGs controllers are capable of voltage and frequency regulation along with controlling active and reactive power sharing among them [3]. While in a grid-connected mode, the main grid regulates MGs' operating frequency and slack bus voltage [4]. In islanded MGs, DGs are interconnected to each other using a suitable control approach for power-sharing (see, for example, [3]–[6]). To design an effective and efficient control strategy, a PF analysis model is required to calculate the steady-state variables, especially for an islanded MG. In popular practices, DG having the highest capacity is considered as a slack bus. This bus operates as an infinite bus at a constant voltage to provide system frequency, and other DGs are treated as either PV or PQ buses. However, this assumption cannot be feasible in Islanded MGs. For example, the generation capacity of DGs is not usually high enough to enable them for acting as an infinite bus [7]. Therefore, a DG cannot be operated as a slack bus in PF analysis. In DCIMGs, load sharing among all DGs has been done using droop controllers. In this case, bus voltage and system frequency are locally regulated [8]. Due to the droop controllers' installation, new PF variables are introduced. These new variables cannot be handled by conventional PF analysis tools.

PF analysis includes computing of bus voltages and line flows in the electric power networks for given load demands. Numerous techniques have been proposed for PF analysis of the different types of electric networks according to

their characteristics. Some of them are derived from the Newton-Raphson (NR) approach [7], [9], while others are based on the basic electric circuit laws [10]. However, conventional algorithms cannot obtain steady-state solutions for the DCIMs due to the droop characteristics of power-sharing controllers. To resolve this issue, Abdelaziz *et al.* proposed a three-phase model of the PF problem as a least-square optimization problem in [11], which adopts the real characteristics of islanded MGs. In [11], the Newton-Trust region (NTR) algorithm is utilized to solve the formulated least-square optimization problem. Although NTR's convergence is better than other conventional techniques, it is highly sensitive to the initial solution. The authors of [12] proposed an interior point-based power flow technique for balanced islanded microgrids, where PF is formulated as COP. However, this algorithm is only applicable to a balanced system. Therefore, this algorithm can hardly be used in the PF analysis since distribution systems are highly unbalanced in nature.

Several modifications to the conventional algorithms have been proposed for increasing their applicability in the case of DCIMGs. Authors of [13] proposed a backward/forward sweep (BFS) method to solve the PF problem of DCIMGs. In [13], a reference voltage is selected from one of the bus voltages of all DGs in such a manner that reactive power generation at other DGs can be regulated. However, this assumption does not mimic the actual behavior of the DCIMGs since reactive power generation depend upon their local bus-voltage magnitude. In [14], a modified BFS algorithm is proposed to obtain steady-state solutions of a DCIMG. However, their application is limited to the radial MGs since BFS algorithms consider the radial structure in their model formulation.

In [15], a modified Gauss-Seidel (GS) algorithm is proposed for PF analysis of the DCIMGs, where all operational features of the DGs are included alongside droop characteristics. Although the PF model is accurate, the modified GS algorithm exhibits poor convergence characteristics as compared to other conventional alternatives. Mumtaz *et al.* [16] propose a Modified NR (MNR) algorithm, where the PF model includes non-linearity of the droop equations. However, MNR fails to converge for the system having a high R/X ratio due to the ill-conditioning of the PF model proposed in [16]. To resolve this issue, Kumar *et al.* [17], [18] proposed a nested iterative framework for the NR-based algorithm to improve the convergence over the PF problem of DCIMGs.

Moreover, several studies based on a nature-inspired optimization algorithm have been performed to solve the PF problem of DCIMGs. The authors of [19] introduced a method based on the Particle Swarm Optimization (PSO) algorithm to solve the PF problem of DCIMGs [19], where PSO is employed to calculate the optimum droop parameters for sharing the reactive power. However, this method cannot consider the sharing of active power among the DGs. In [20],

the work of [19] is extended by implementing two operators, mutation and guaranteed convergence, in PSO. These operators improve accuracy and ability to drag solutions from the infeasible regions to feasible regions. A Genetic Algorithm (GA) based PF models for DCIMGs is also proposed in [21], and [22]. A new hybrid evolutionary algorithm is proposed in [23] where hybridization of two different evolutionary algorithms (GA and Imperialist Comparative Algorithm (ICA)) is done and named as Imperialist comparative algorithm and genetic algorithm (ICGA). However, solutions obtained by these evolutionary algorithms are not so accurate for considering as a steady-state solution.

Moreover, PF problems can be divided into three classes i) well-conditioned, ii) ill-conditioned, and iii) unsolvable. In the well-conditioned case, conventional PF algorithms, such as Newton's based algorithm, can easily solve under the flat initial seed. Although ill-conditioned PF problems are solvable, traditional algorithms fail to converge under the flat start. Usually, the real operating point of these problems is far away from the flat start. On the other hand, the unsolvable PF problem has no solution in its feasible region. In the case of DCIMG, ill-conditioned and unsolvable systems are frequently encountered. PF algorithms may fail to converge for some ill-conditioned operating conditions of the DCIMG, such as heavy load, faulty lines, etc. A robust PF method should have the following qualities.

1) It must show high efficiency while solving well-conditioned test cases.
2) It must provide adequate robustness towards the ill-conditioned conditions.
3) It can obtain a PF solution for unsolvable cases near to a feasible operating state.

However, to achieve the above-mentioned properties, a balance between convergence and efficiency is expected in the core of the PF methods during the iterative steps. In Table 1, a summary of recently proposed power flow algorithms for microgrids is reported. As shown in the Table 1, ill-conditioned and unsolvable test cases have not been considered. In this work, a global convergent PF algorithm is proposed that provide effective and robust performance over different kind of PF problems: i) well-conditioned microgrids, ii) ill-conditioned microgrids, and iii) unsolvable microgrids.

To overcome all the above-discussed limitations of state-of-the-art algorithms, this paper proposes a new PF formulation expressed in the form of the COP, where different modes of operations of DGs, such as PV, PQ, and droops operations are modeled as problem constraints. To solve this COP, a novel optimization algorithm, called ϵDE-NGM, is proposed. The convergence capability and feasibility related issues of DE are improved for solving the COPs having a high number of equality constraints. For this purpose, a solution repairing mutation operator, called NGM, is incorporated in DE to repair an infeasible solution. The performance of

TABLE 1. A summary of major power flow algorithms of islanded MG proposed since last decade. Ref.: Reference, IM: Islanded Microgrid, GCM: Grid-connected Microgrid,, BO: Balanced Operation, UBO: Unbalanced Operation, MN: Meshed Network, RN: Radial Network, IC: Ill-conditioned, US: Unsolvable Case.

Ref.,year	IM/GCM	BO/UBO	MN/RN	IC	US
Optimization based power flow algorithm					
[11], 2012	IM	BO & UBO	RN	✗	✗
[23], 2016	IM	BO	RN	✗	✗
[12], 2016	IM	BO	RN	✗	✗
[20], 2016	IM	BO & UBO	RN	✗	✗
[24], 2017	IM	BO & UBO	RN	✗	✗
[25], 2020	IM	BO & UBO	RN	✗	✗
[26], 2021	IM	BO	RN	✗	✗
This work	IM & GCM	BO & UBO	MN & RN	✓	✓
Jacobian based power flow algorithm					
[16], 2015	IM	BO	RN	✗	✗
[27], 2018	IM	BO & UBO	RN	✗	✗
[28], 2019	IM	BO	MN & RN	✗	✗
[18], 2019	IM	BO	RN	✓	✗
[29], 2020	IM	BO	RN	✗	✗
[17], 2020	IM	BO	RN	✓	✗
[30], 2020	IM	BO	RN	✓	✗
[31], 2021	IM & GCM	BO & UBO	MN & RN	✓	✗
Non-Jacobian based power flow algorithm					
[13], 2015	IM	BO	RN	✗	✗
[32], 2017	IM	BO	RN	✗	✗
[33], 2017	IM	BO	RN	✗	✗
[34], 2018	IM & GCM	BO & UBO	RN	✗	✗
[35], 2018	IM	BO	RN	✗	✗
[14], 2019	IM	BO	MN & RN	✗	✗
[36], 2019	IM & GCM	BO & UBO	RN	✗	✗
[37], 2020	IM	BO	RN	✗	✗
[38], 2020	IM	BO	RN	✗	✗

ϵDE-NGM is analysed over modern COPs, and obtained results are compared with the results of state-of-the-art algorithms to show the algorithm's effectiveness. Furthermore, to show the efficacy of the ϵDE-NGM as a PF tool, a comparative analysis with the time domain simulator in PSCAD [39], evolutionary algorithms methods (GPSO-GM [20], and ICGA [23]) and deterministic method, i.e., NTR [11] are also presented. The main contributions of this work are summarized as follows.

- A novel formulation is introduced as a COP for the PF analysis of DCIMGs.
- This PF formulation includes constraints based on the droop characteristics of DGs to deal with the droop buses. Besides, system frequency is also considered as an extra variable of the PF problem.
- A metaheuristic, named as ϵDE-NGM, is proposed to solve COPs with non-linear equality constraints. Moreover, this algorithm is utilized as a PF tool for DCIMGs by solving the PF problem formulated as a COP.
- This PF solving approach implements an adequate method to share reactive and active power among DGs based on their droop characteristics.

This paper is organized as follows. In the second section, the microgrid system and load are modeled. This is followed by formulating the constrained optimization problem for a power flow analysis of islanded MGs. In the fourth section,

the main steps of the optimization algorithm are proposed. The validation of the proposed algorithm on the power flow problem of islanded MGs is discussed in the fifth section. Finally, the conclusion of this paper is given in section six.

II. DIFFERENTIAL EVOLUTION

DE is a global optimization search algorithm proposed by Storn and Price [40]. DE can be applied to different optimization problems *viz.* non-convex, non-differential, non-linear, and multi-modal problems. In literature, it is shown that DE has been proved to be robust and efficient in these problems [41]. In DE, initial solutions are generated randomly within the lower and upper bound of search space, and these solutions form an initial population. Each solution consists of *n* elements as decision parameters of the problem. At each iteration, all solutions of the population are selected as parents. Offspring generation of each parent is done as follows:

- The mutation process begins with the selection of 3 solutions from the population different from the parent. The first solution out of 3 is considered a base vector and the other two solutions are utilized to generate a difference vector. This difference vector is weighted using a parameter *F* and added to the base vector. This process returns a vector, called a mutant vector, for each parent.
- The mutant vectors crossover with their parent solutions to generate trial solutions. Here, the probability of crossover is controlled by a parameter *CR*. This scheme returns a trial solution for each parent solution.
- Finally, the trial solutions are compared one-yo-one with their parent, where a trial solution is selected in place of its parent if it is better than the parent in terms of fitness value.

The DE [40] algorithm is a popular global optimization technique used in different problems of the power system. DE is a more robust and efficient technique as compared with other evolutionary algorithms (EAs). Enhanced variants of DE have been considered the best according to recent CEC competitions [42], [43]. However, most power system problems contain several constraints, and DE may not be directly applied to such problems. To cope with this issue, several variants of DE have been proposed in the literature. To solve COPs, a modified variant of DE is proposed in [44], where multiple trial solutions are generated for each individual using various mutation operators. Deb's feasibility rule [45] is employed in the selection procedure to handle the constraints.

Elsayed *et al.* [46] proposed a multi-operator based self-adaptive DE to solve COPs. In that paper, each mutation operator has its own sub-population to generate new trial solutions. An improvement index is utilized to dynamically change the number of individuals in each sub-population according to their success rate. In [47], an improved version of the above-discussed algorithm, called ISAMODE-CMA, is proposed, where the CMA-ES algorithm is utilized as

a local search operator, and a dynamic penalty is used to transform constrained-space into bound-constrained-space of the given problems. In [48], a multi-operator based DE variant is proposed where two crossover operators, four mutation strategies, and two constraint handling techniques are incorporated in DE's framework to solve COPs.

Wang *et al.* [49] proposed a composite DE for solving COPs using three distinct mutation operators. Each mutation operator generates trial solutions for each solution where one operator is used to improve diversity, while others increase the convergence rate. Furthermore, a hybrid constraint handling technique and restart mechanism are also developed to handle the COPs' complex constraints. In [50], an adaptive DE algorithm is proposed to solve COPs, where DE/rand/1/bin mutation strategy is applied in the early stage of optimization. In contrast, DE/rand/1/exp mutation strategy is utilized in later iterations. Division of optimization stages and applying different mutation strategies in each stage improve the balance between exploitive and exploratory search. Moreover, CR is dynamically updated using the success information of generated individuals.

Gao *et al.* [51] proposed a dual-population based DE variant with coevolution for constrained optimization. In that algorithm, a COP is transformed into a bi-objective optimization problem where the first objective is the actual objective function, and another one is the constraint violation. The whole population is divided into two sub-populations in which each sub-population is evolved to improve respective objectives. An information-sharing scheme is also proposed to exchange the information between these sub-populations. In [52], an improved variant of DE is proposed to solve COPs, where one of two distinct mutation operator is selected randomly to improve the solution quality in the population. Moreover, to deal with equality constraints, a new scheme is proposed to transform equality constraints into inequality constraints.

Trivedi *et al.* [53] proposed a unified DE (IUDE) algorithm for constrained optimization, where existing DE variants, SaDE, CoDE, and JADE with the ranking based mutation are incorporated in a single framework. In that algorithm, three mutation strategies and two-parameter settings with static penalty technique are used to evolve two sub-populations. An enhanced variant of IUDE is introduced in [54], where a combination of Deb's feasibility rule and ϵ-constrained are applied to deal with constraints. Interested readers can pursue a review paper written by Das *et al.* [55] for further information about the new improvements of DE. In the literature, numerous DE-based algorithms have been proposed to solve COPs. However, existing algorithms suffer from serious issues, which are as follows [56].

1) The performance of the above-mentioned algorithms deteriorates when the number of equality constraints increases.
2) The above-mentioned algorithms may not find a feasible solution to problems having a low volume of feasible regions.

3) They can suffer from local convergence when multiple disconnected feasible regions are present in the problem-space.

Generally, power system planning problems involve many equality constraints, and identifying a feasible solution becomes extremely challenging for state-of-the-art algorithms [57]. For dealing with the equality constraints, most of the EAs convert equality constraints into relaxed inequality constraints. As a result, the feasibility of the obtained solutions is inadequate. To address this issue, this paper introduces an algorithm to solve the problem with many equality constraints by introducing a NGM operator that finds a feasible solution from an infeasible solution using the NG [58] algorithm at the infeasible solution as an initial solution. The proposed algorithm is named as ϵDE-NGM, and the main operators of ϵDE-NGM are discussed in the next section.

III. PROPOSED ALGORITHM
This section introduces the proposed algorithm ϵDE-NGM, which utilizes ϵ-constrained and NGM to handle the constraints for solving COPs with a large number of equality constraints.

Without losing generality, a COP can be defined as follows.

$$\text{Minimize}, f(\bar{x})$$
$$\text{subject to: } g_i(\bar{x}) < 0, \ i = 1, 2, \ldots, ng,$$
$$h_j(\bar{x}) = 0, \ j = 1, 2, \ldots, nh,$$
$$\bar{x}_L \leq \bar{x} \leq \bar{x}_U. \tag{1}$$

Degree of the constraint violation, $\phi(\bar{x})$, can be calculated as follows:

$$\phi(\bar{x}) = \frac{\sum_{i=1}^{ng} \max\{0, g_i(\bar{x})\} + \sum_{j=1}^{nh} \max\{0, |h_j(\bar{x})| - \epsilon\}}{nh + ng}, \tag{2}$$

where ϵ is equal to 0.0001.

A. GAUSS-NEWTON BASED MUTATION
The NGM is an operator used to calculate a feasible solution for an infeasible solution using gradient information of constraints. In this operator, the infeasibility of the solution is considered a least-square optimization problem. This least square problem is solved using the Gauss-Newton algorithm [58]. The infeasibility of the solution, $\Phi(\bar{x})$, can be represented as a least-square optimization problem using the following equation.

$$\Phi(\bar{x}) = 0.5 \left(\sum_{i=1}^{ng} \max\{0, g_i(\bar{x})\}^2 + \sum_{j=1}^{nh} h_j(\bar{x})^2 \right) \tag{3}$$

In GNM, this problem is solved using iterative Newton-Gauss algorithm. $\triangle \bar{x}$, are defined as follows [58].

$$\triangle \bar{x} = -\frac{\nabla C(\bar{x})^T \triangle C(\bar{x})}{\nabla C(\bar{x})^T \nabla C(x)}, \tag{4}$$

where,

$$\triangle C(\bar{x}) = [\triangle g_1(\bar{x}) \ldots \triangle g_{ng}(\bar{x}), \triangle h_{ng+1}(\bar{x}) \ldots \triangle h_{ng+nh}(\bar{x})]^T,$$
$$\triangle g_i(\bar{x}) = max\{0, g_i(\bar{x})\}. \tag{5}$$

This mutation operation, $\bar{x}^{fea} = \bar{x}^{infea} + \triangle\bar{x}^{infea}$, is executed in iterative fashion when $\bar{x}^{infea}$ is infeasible solution. This mutation operation is repeated for N_g times while the solution infeasible.

B. ϵ-CONSTRAINED HANDLING TECHNIQUE
In ϵ-constraint handling technique, an ϵ-level comparison is done to compare the solutions [59]. The ϵ-level comparison is defined using lexicographic order in which constraint violation, $\phi(\bar{x})$, precedes objective function value, $f(\bar{x})$ [59].

Let $\{\phi_1, \phi_2\}$ and $\{f_1, f_2\}$ be the constraint violation value and the function value at points $\{x_1, x_2\}$ respectively. Then, the ϵ level comparisons are defined as follows.

$$(f_2, \phi_2) <_\epsilon (f_1, \phi_1) \Leftrightarrow \begin{cases} f_2 < f_1, & \text{if } (\phi_1, \phi_1 \leq \epsilon) \\ f_2 < f_1, & \text{if } (\phi_1 == \phi_2) \\ \phi_2 < \phi_1, & \text{otherwise}, \end{cases} \tag{6}$$

$$(f_2, \phi_2) \leq_\epsilon (f_1, \phi_1) \Leftrightarrow \begin{cases} f_2 \leq f_1, & \text{if } (\phi_1, \phi_1 \leq \epsilon) \\ f_2 \leq f_1, & \text{if } (\phi_1 == \phi_2) \\ \phi_2 \leq \phi_1, & \text{otherwise}. \end{cases} \tag{7}$$

Generally, there is no need to control ϵ-level for most of the COPs. However, COPs with equality constraints should be solved by controlling the ϵ level during the optimization. A simple way to control the ϵ-level is proposed in [59] and defined using the following equations.

$$\epsilon(t) = \begin{cases} \phi(\bar{x}_\theta)(1 - \frac{t}{T_c})^{cp}, & 0 < t < T_c \\ 0, & T_c \leq t. \end{cases} \tag{8}$$

C. THE ALGORITHM ϵDE-NGM
The algorithm ϵDE-NGM is based on DE/rand/1/exp. The main steps of algorithm ϵDE-NGM are shown in Fig. 1.

- **Step 1:** *Initialization-* In this step, a population, P, of N_p solutions is initialized within the bound of search-space using the following equation.

$$\bar{x}_i^0 = (\bar{x}_U - \bar{x}_L)rand + \bar{x}_L, \ i = 1, 2, \ldots N, \tag{9}$$

where *rand* represents the random number generator which generates the number from uniform distribution within the range (0, 1). An initial value of ϵ-level, $\epsilon(0)$, is calculated using (8).

- **Step 2:** *Mutation-* For each solution $\bar{x}_i^k$, three different solution $\bar{x}_{r1}^k$, $\bar{x}_{r2}^k$, and $\bar{x}_{r3}^k$ are selected from the current population. A new mutant solution, $\bar{v}_i^k$, is calculated using $\bar{x}_{r1}^k$, $\bar{x}_{r2}^k$, and $\bar{x}_{r3}^k$ as follows.

$$\bar{v}_i^k = \bar{x}_{r1}^k + sF(\bar{x}_{r2}^k - \bar{x}_{r3}^k), \tag{10}$$

- **Step 3:** *Crossover-* The mutant solution v_i^k, is used as a donor solution in crossover operation of solution x_i^k to generate a trial solution, u_i^k. A crossover point, l,
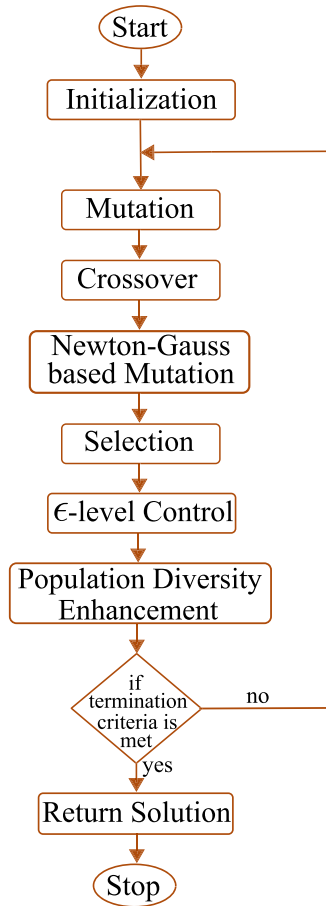
FIGURE 1. Flowchart of the ϵDE-NGM.

is randomly selected from 1 to D. The elements of $l - th$ dimension of the trail solution u_i^k is taken from the element of $l - th$ dimension of donor solution v_i^k. Subsequent elements of trial solution u_i^k are taken from donor solution v_i^k with exponentially decreasing probability (calculated using crossover rate CR). Rest of the elements of trial solution u_i^k are taken from the elements of solution x_i^k.

- **Step 4:** *Newton-Gauss based Mutation-* If the generated trial solution u_i^k is infeasible (does not satisfy all the constraints), u_i^k is updated using NGM. This process is repeated until the number of trials of NGM reaches to N_g or solution u_i^k becomes a feasible solution.
- **Step 5:** *Selection-* If the trial solution u_i^k is better than solution x_i^k on the basis of ϵ-level comparison, the trial solution u_i^k is replaced the solution x_i^k for the next iteration.
- **Step 6:** *ϵ-level control-* The value of ϵ-level is updated using (8).
- **Step 7:** *Population Diversity Enhancement-* To cope with premature convergence and stagnation, population diversity is improved using reinitialization of the population. Reinitialization of the population is done when

one of the following two criteria is fulfilled during the search.

1) Population diversity becomes very low ($< 10^{-8}$).
2) Standard deviation of the degree of constrained violation of the population becomes very low ($< 10^{-8}$), and a feasible solution is not existing in that population.

- **Step 8:** *Termination Condition-* If the total number of iterations becomes greater than the maximum allowed iteration (T_{max}), the algorithm is terminated. Otherwise, go to **Step 2**.

D. GLOBAL CONVERGENCE PROPERTY OF THE ϵDE-NGM

In this section, the proposed algorithm's asymptotic global convergence is verified using several theoretical concepts and statements. Here asymptotic global convergence means that when the number of iteration satisfies $t \rightarrow \infty$ then the probability of the algorithm's best solution is global optimum approaches 1.

To verify the global convergence property of the proposed algorithm, the convergence concept in probability is introduced here as defined in [60].

Definition 1: Let assume a population sequence of each iteration, $\{\mathbf{Y}(1), \mathbf{Y}(2), \ldots \mathbf{Y}(k)\}$, generated by the proposed algorithm to solve a constrained optimization problem. Then, the proposed algorithm converges to a feasible solution set in probability if it satisfies the following condition.

$$\lim_{k \to \infty} p\{\mathbf{Y}(k) \cap \mathcal{S}^* \neq \emptyset\} = 1, \tag{11}$$

where $\mathcal{S}^*$ represents the solution set of the feasible optimal solutions and p is the probability of occurrence of an event.

Theorem 1: Let an individual y exists in each population $\mathbf{Y}(k)$ such that

$$p\{y \in \mathcal{S}^*\} \geq \alpha > 0. \tag{12}$$

Here α is a positive number, then the proposed algorithm can converge to a solution of the optimal solution set in terms of probability.

Proof: The probability of a population's solution be the element of the optimal solution set can be calculated using the following relation.

$$p\{y_i^k \in \mathcal{S}^*\} = \frac{\mu(\mathcal{S}^*)}{\mu(\mathbf{Y}(k))} \frac{\mid \sigma(\mathbf{Y}(k)) \mid}{\max\{\mid y_i^k - \mathbf{E}(\mathcal{S}^*) \mid, \mid \sigma(\mathbf{Y}(k)) \mid\}}, \tag{13}$$

where $\mu()$ represents the Lebesgue measure, $E()$ represents the expected or mean value, and $\sigma()$ represents the standard deviation value. As the population is reinitialized when it converges to the non-optimal point, $p\{y_i^k \in \mathcal{S}^*\}$ is always greater than zero, i.e.

$$p\{y_i^k \in \mathcal{S}^*\} = \alpha_i^k > 0. \tag{14}$$

Therefore,

$$p\{\mathbf{Y}(k) \cap \mathcal{S}^* = \emptyset\} = 1 - \alpha_{max}^k, \tag{15}$$

where,

$$\alpha_{max}^k = \max\{\alpha_1^k, \alpha_2^k, \cdots, \alpha_{N_p}^k\}. \tag{16}$$

In DE, the current population's best solution is the same or better than the best solution of the population obtained in previous iterations, implying

$$\lim_{k\to\infty} p\{\mathbf{Y}(k) \cap \mathcal{S}^* \neq \emptyset\} = \lim_{k\to\infty} 1 - \prod_{i=1}^k (1 - \alpha_{max}^k) = 1, \tag{17}$$

which is required to prove. □

IV. POWER FLOW FORMULATION

In this section, the PF problem of the DCIMG is described. Then, this problem is transformed into a COP to apply evolutionary algorithms to solve the PF problem of DCIMGs. The modeling of the DCIMG and it's components is an important action that influences the PF solutions. The DG and load models are presented in the following subsection.

A. MODELING OF THE DCIMG AND IT'S COMPONENTS
1) STATIC LOAD MODEL
In the static load model, active and reactive power absorbed by the load depends upon the bus voltage and system frequency.

$$P_{l,k} = P_{0,l,k}(a_p + b_p|V_k| + c_p|V_k|^2 + d_p|V_k|^\alpha)$$
$$\times (1 + e_p(\omega - \omega_0)), \tag{18}$$
$$Q_{l,k} = Q_{0,l,k}(a_q + b_q|V_k| + c_q|V_k|^2 + d_q|V_k|^\beta)$$
$$\times (1 + e_q(\omega - \omega_0)), \tag{19}$$

where $a_p + b_p + c_p + d_p = 1$; $a_q + b_q + c_q + d_q = 1$.

Voltage and frequency-based active and reactive loads can be represented using (18) and (19) respectively as reported in [14], [61].

2) MODELING OF LINES IN ISLANDED MGs
A line impedance of islanded MGs can be defined as, $z = r + jwl$. Here, the value of reactance, $x (= wl)$, depends on the operating frequency. Therefore, small deviation in frequency can change the reactance of the lines.

3) MODELING OF DGs IN CASE OF ISLANDED MGs
In grid-connected MGs, DGs can provide pre-specified active and reactive generation to satisfy system loads' power demands. In such an operation, the difference in total load demand and power generated by DGs are supplied or absorbed by the main grid to kept the system frequency and voltages of the buses constant. Similar to conventional power systems, in grid-connected MGs, DGs can be modeled as a PV, and PQ bus [62], [63]. However, this cannot be valid in the case of DCIMGs due to the following reasons.

1) There is no slack bus in DCIMGs.
2) System frequency is not constant.

3) Reference voltage does not exist in islanded MGs to calculate the voltage of all system buses.
4) In an islanded mode, the deviation between power generation and demands may be fixed by changing the system frequency and magnitude of the voltage using droop controllers.

Therefore, islanded MGs' power flow problem will be solved without considering the slack bus in the system. To formulate the power flow problem of islanded MGs, in place of a slack bus, multiple droop buses are modeled based on the droop characteristics to share the power demand among the DGs. According to the controllers' droop characteristics, an increment in reactive power and active power demand follows from a decrement in the magnitude of the voltage and operating frequency, respectively. So, in the case of droop bus, reactive and active power generation of a DG can be calculated using the following equations.

$$P_i = \frac{1}{np_i}(w_i^* - w), \tag{20}$$

$$Q_i = \frac{1}{mq_i}(V_i^* - V_i), \tag{21}$$

where V_i^* and w_i^* represent the nominal values of voltage magnitude and frequency, respectively; Based on the IEEE Standard 1547.7 [4], (20) and (21) are valid for islanded MGs where the output impedance of converter is assumed inductive.

B. POWER FLOW EQUATIONS
In DCIMGs, the operating frequency is an extra unknown variable of the PF problem. Therefore, new equations should be derived for the PV, PQ, and droop buses presented below.

1) PF EQUATIONS OF A DROOP BUS
The value of active and reactive power injection of bus i can be defined using the following equations.

$$P_i = P_{i,dg} - P_{i,l}, \tag{22}$$
$$Q_i = Q_{i,dg} - Q_{i,l}, \tag{23}$$

where $P_{i,dg}$ and $Q_{i,dg}$ are calculated using (20) and (21). Here, P_i and Q_i can be calculated using following equations.

$$P_i = V_{ri}\sum_{j=1}^N (V_{rj}G_{ij} - V_{mj}B_{ij}) + V_{mi}\sum_{j=1}^N (V_{rj}B_{ij} + V_{mj}G_{ij}), \tag{24}$$

$$Q_i = V_{mi}\sum_{j=1}^N (V_{rj}G_{ij} - V_{mj}B_{ij}) - V_{ri}\sum_{j=1}^N (V_{rj}B_{ij} + V_{mj}G_{ij}). \tag{25}$$

2) PF EQUATIONS OF A PQ BUS

The active and reactive power injection are known in PQ buses, so PQ buses can be defined as follows.

$$P_k = V_{rk} \sum_{j=1}^{N}(V_{rj}G_{kj} - V_{mj}B_{kj}) + V_{mk} \sum_{j=1}^{N}(V_{rj}B_{kj} + V_{mj}G_{kj}),$$
(26)

$$Q_k = V_{mk} \sum_{j=1}^{N}(V_{rj}G_{kj} - V_{mj}B_{kj}) - V_{rk} \sum_{j=1}^{N}(V_{rj}B_{kj} + V_{mj}G_{kj}).$$
(27)

3) PF EQUATIONS OF A PV BUS

The active power and voltage magnitude are known in PV buses, so PV buses can be defined as follows.

$$P_k = V_{rk} \sum_{j=1}^{N}(V_{rj}G_{kj} - V_{mj}B_{kj}) + V_{mk} \sum_{j=1}^{N}(V_{rj}B_{kj} + V_{mj}G_{kj}),$$
(28)

$$V_k^2 = V_{rk}^2 + V_{mk}^2.$$
(29)

C. POWER FLOW PROBLEM FORMULATION AS A CONSTRAINED OPTIMIZATION PROBLEM

To solve the PF problem of DCIMGs, a COP is derived.

1) OBJECTIVE FUNCTION

Here, the impact of droop equations defined in (20) and (21) on PF solutions is exercised in the objective function. Therefore, the objective function is to minimize the sum of square error of mismatch equations of droop bus i.e.

$$f = \sum_{k \in S_{dg}}(\triangle P_k^2 + \triangle Q_k^2),$$
(30)

where

$$\triangle P_k = \frac{1}{np_k}(w_i^* - w) - P_{k,dg},$$
(31)

$$\triangle Q_k = \frac{1}{mq_k}(V_k^* - V_k) - Q_{k,dg},$$
(32)

In this formulation, PF equations are considered as equality constraints.

1) Equality constraints related to kth PQ or Droop bus.

$$P_k - V_{rk} \sum_{j=1}^{N}(V_{rj}G_{kj} - V_{mj}B_{kj}) - V_{mk} \sum_{j=1}^{N}$$
$$(V_{rj}B_{kj} + V_{mj}G_{kj}) = 0,$$
(33)

and

$$Q_k - V_{mk} \sum_{j=1}^{N}(V_{rj}G_{kj} - V_{mj}B_{kj}) + V_{rk} \sum_{j=1}^{N}$$
$$(V_{rj}B_{kj} + V_{mj}G_{kj}) = 0.$$
(34)

2) Equality constraints related to kth PV bus.

$$P_k - V_{rk} \sum_{j=1}^{N}(V_{rj}G_{kj} - V_{mj}B_{kj})$$
$$- V_{mk} \sum_{j=1}^{N}(V_{rj}B_{kj} + V_{mj}G_{kj}) = 0,$$
(35)

and

$$V_k^2 - V_{rk}^2 - V_{mk}^2 = 0.$$
(36)

3) Bound constraints.

$$V_{rk,min} \leq V_{rk} \leq V_{rk,max}, \quad k = 1, 2, \ldots, Nbus,$$
$$V_{mk,min} \leq V_{mk} \leq V_{mk,max}, \quad k = 1, 2, \ldots, Nbus,$$
$$w_{min} \leq w \leq w_{max},$$
$$P_{j,min} \leq P_{j,dg} \leq P_{j,max}, \quad j \in S_{dg},$$
and
$$Q_{j,min} \leq Q_{j,dg} \leq Q_{j,max}, \quad j \in S_{dg}$$
(37)

In DCIMG system having N buses and M DGs, total number of variables is $(2N + 2M)$ and number of equality constraints is $2N$.

V. RESULT AND DISCUSSIONS

To investigate the performance of the ϵDE-NGM, two sets of problems are utilized. The first one includes 28 benchmark problems with different scales taken from the IEEE CEC 2017 [64]. The second one includes PF problems of different test systems. These problems contain different hard properties, such as small and separated feasible regions, strong nonlinearity, and rotated search space.

A. EXPERIMENT 1: BENCHMARK ON IEEE CEC 2017 PROBLEM SUITE

In this experiment, parameter settings such as population size and maximum allowed function evaluations are reported in Table. 2. 25 independent runs is performed on each test problem of IEEE CEC 2017's test-suite. It is worth noting that maximum function evaluations allowed is set according to guidelines provided in [64], and the same setting is also used in other algorithms used in comparative analysis.

TABLE 2. Population Size N_p and Maximum allowed function evaluations Max_{FEs}.

Test Problems	N_p	Max_{FEs}
10-D	35	2.00E+05
30-D	50	6.00E+05
50-D	50	1.00E+06
100-D	50	2.00E+06

The performance of ϵDE-NGM is compared with five state-of-the-art algorithms, such as ϵMAgES [65], IUDE [54], ϵLSHADE44 [66], CORCO [67], and DECODE [68].

TABLE 3. Experimental outcomes of εDE-NGM and five selected contenders over 25 independent runs on the 28 test problems with dimension 10 from IEEE CEC 2017.

Prob	εDE-NGM OF	εDE-NGM CV	εMAg-ES OF	εMAg-ES CV	W	IUDE OF	IUDE CV	W	εLSHADE44 OF	εLSHADE44 CV	W	CORCO OF	CORCO CV	W	DECODE OF	DECODE CV	W
1	**0.00E+00**	**0.00E+00**	1.65E-30	0.00E+00	+	**0.00E+00**	**0.00E+00**	=	**0.00E+00**	**0.00E+00**	=	**0.00E+00**	**0.00E+00**	=	**0.00E+00**	**0.00E+00**	=
2	**0.00E+00**	**0.00E+00**	**0.00E+00**	**0.00E+00**	=	**0.00E+00**	**0.00E+00**	=	**0.00E+00**	**0.00E+00**	=	**0.00E+00**	**0.00E+00**	=	**0.00E+00**	**0.00E+00**	=
3	**0.00E+00**	**0.00E+00**	4.73E-31	0.00E+00	+	3.54E+01	0.00E+00	+	5.93E+01	0.00E+00	+	**0.00E+00**	**0.00E+00**	=	**0.00E+00**	**0.00E+00**	=
4	**1.36E+01**	**0.00E+00**	2.98E+01	0.00E+00	+	5.00E+00	0.00E+00	-	**1.36E+01**	**0.00E+00**	=	1.37E+01	0.00E+00	+	**1.36E+01**	**0.00E+00**	=
5	**0.00E+00**	**0.00E+00**	**0.00E+00**	**0.00E+00**	=	1.74E-30	0.00E+00	+	**0.00E+00**	**0.00E+00**	=	**0.00E+00**	**0.00E+00**	=	**0.00E+00**	**0.00E+00**	=
6	**0.00E+00**	**0.00E+00**	3.58E+01	0.00E+00	+	**0.00E+00**	**0.00E+00**	=	1.69E+01	2.07E-03	+	**0.00E+00**	**0.00E+00**	=	**0.00E+00**	**0.00E+00**	=
7	-4.27E+02	0.00E+00	-3.17E+02	0.00E+00	+	-2.77E+02	2.10E-04	+	-1.21E+02	0.00E+00	+	-4.46E+01	0.00E+00	+	**-4.65E+02**	**0.00E+00**	-
8	**-1.35E-03**	**0.00E+00**	**-1.35E-03**	**0.00E+00**	=	**-1.35E-03**	**0.00E+00**	=	**-1.35E-03**	**0.00E+00**	=	**-1.35E-03**	**0.00E+00**	=	**-1.35E-03**	**0.00E+00**	=
9	**-4.98E-03**	**0.00E+00**	**-4.98E-03**	**0.00E+00**	=	**-4.98E-03**	**0.00E+00**	=	**-4.98E-03**	**0.00E+00**	=	-3.04E-02	4.97E-02	+	**-4.98E-03**	**0.00E+00**	=
10	**-5.10E-04**	**0.00E+00**	**-5.10E-04**	**0.00E+00**	=	**-5.10E-04**	**0.00E+00**	=	**-5.10E-04**	**0.00E+00**	=	**-5.10E-04**	**0.00E+00**	=	**-5.10E-04**	**0.00E+00**	=
11	-1.63E-01	0.00E+00	-1.68E-01	0.00E+00	=	-1.57E-01	0.00E+00	+	**-1.69E-01**	**0.00E+00**	-	-4.83E+02	4.70E+02	+	-2.20E+00	1.56E-07	+
12	**3.99E+00**	**0.00E+00**	7.00E+00	0.00E+00	+	**3.99E+00**	**0.00E+00**	=	**3.99E+00**	**0.00E+00**	=	5.13E+00	0.00E+00	+	**3.99E+00**	**0.00E+00**	=
13	**0.00E+00**	**0.00E+00**	1.59E-01	0.00E+00	+	**0.00E+00**	**0.00E+00**	=	2.82E+00	0.00E+00	+	**0.00E+00**	**0.00E+00**	=	1.59E-01	0.00E+00	+
14	**2.38E+00**	**0.00E+00**	2.87E+00	7.94E-02	+	**2.38E+00**	**0.00E+00**	=	2.39E+00	0.00E+00	+	3.02E+00	4.41E-02	+	**2.38E+00**	**0.00E+00**	=
15	**2.36E+00**	**0.00E+00**	7.61E+00	2.86E-02	+	6.38E+00	0.00E+00	+	2.86E+00	2.75E-04	+	2.36E+00	2.42E-06	+	**2.36E+00**	**0.00E+00**	=
16	**0.00E+00**	**0.00E+00**	**0.00E+00**	**0.00E+00**	=	**0.00E+00**	**0.00E+00**	=	**0.00E+00**	**0.00E+00**	=	**0.00E+00**	**0.00E+00**	=	1.76E+00	0.00E+00	+
17	**2.82E-02**	**4.50E+00**	7.35E-01	5.85E+00	+	1.99E-02	4.54E+00	+	5.28E-01	4.50E+00	+	1.24E-02	4.51E+00	+	5.70E-02	4.50E+00	+
18	3.67E+01	0.00E+00	**3.66E+01**	**0.00E+00**	=	9.48E+00	1.33E+01	+	3.67E+01	0.00E+00	=	1.33E+00	8.29E-01	+	6.13E+03	9.38E+07	+
19	4.06E-04	6.63E+03	1.12E+00	6.63E+03	+	**0.00E+00**	**6.63E+03**	-	**0.00E+00**	**6.63E+03**	-	-5.88E+00	6.64E+03	+	4.00E-03	6.63E+03	+
20	**5.21E-01**	**0.00E+00**	1.17E+00	0.00E+00	+	6.49E-01	0.00E+00	+	6.18E-01	0.00E+00	+	5.41E-01	0.00E+00	+	6.49E-01	0.00E+00	+
21	**3.99E+00**	**0.00E+00**	4.41E+00	0.00E+00	+	**3.99E+00**	**0.00E+00**	=	**3.99E+00**	**0.00E+00**	=	3.68E+01	0.00E+00	+	**3.99E+00**	**0.00E+00**	=
22	**0.00E+00**	**0.00E+00**	6.38E-01	0.00E+00	+	2.98E+00	0.00E+00	+	1.12E+00	0.00E+00	+	**0.00E+00**	**0.00E+00**	=	4.78E-01	0.00E+00	+
23	2.51E+00	0.00E+00	2.50E+00	9.45E-04	=	**2.38E+00**	**0.00E+00**	-	2.39E+00	0.00E+00	-	4.03E+00	5.34E+02	+	**2.38E+00**	**0.00E+00**	-
24	**2.36E+00**	**0.00E+00**	6.13E+00	0.00E+00	+	5.50E+00	0.00E+00	+	2.86E+00	9.99E-05	+	2.35E+00	2.82E-05	+	**2.36E+00**	**0.00E+00**	=
25	**0.00E+00**	**0.00E+00**	**0.00E+00**	**0.00E+00**	=	**0.00E+00**	**0.00E+00**	=	1.01E+00	0.00E+00	+	**0.00E+00**	**0.00E+00**	=	2.32E+00	0.00E+00	+
26	6.89E-01	4.50E+00	7.54E-01	5.42E+00	+	8.65E-02	4.79E+00	+	7.73E-01	5.02E+00	+	5.95E-01	5.53E+00	+	**5.46E-02**	**4.50E+00**	-
27	3.46E+01	0.00E+00	7.59E+01	0.00E+00	+	7.67E+01	2.89E+02	+	3.66E+01	0.00E+00	+	1.92E+01	6.05E+01	+	2.20E+04	8.87E+08	+
28	3.90E+00	6.64E+03	8.68E+00	6.64E+03	+	4.57E+00	6.64E+03	+	2.88E+01	6.65E+03	+	-4.38E+02	6.64E+03	+	**4.49E-03**	**6.63E+03**	-
+/=/-				19/9/0			13/12/3			14/11/3			17/11/0			10/14/4	

TABLE 4. Experimental outcomes of εDE-NGM and five selected contenders over 25 independent runs on the 28 test problems with dimension 30 from IEEE CEC 2017.

Prob	εDE-NGM OF	εDE-NGM CV	εMAg-ES OF	εMAg-ES CV	W	IUDE OF	IUDE CV	W	εLSHADE44 OF	εLSHADE44 CV	W	CORCO OF	CORCO CV	W	DECODE OF	DECODE CV	W
1	**0.00E+00**	**0.00E+00**	3.75E-28	0.00E+00	+	4.13E-29	0.00E+00	+	5.70E-30	0.00E+00	+	**0.00E+00**	**0.00E+00**	=	**0.00E+00**	**0.00E+00**	=
2	**0.00E+00**	**0.00E+00**	3.76E-28	0.00E+00	+	4.42E-29	0.00E+00	+	6.06E-30	0.00E+00	+	**0.00E+00**	**0.00E+00**	=	**0.00E+00**	**0.00E+00**	=
3	**0.00E+00**	**0.00E+00**	6.73E-28	0.00E+00	+	1.29E+02	0.00E+00	+	7.19E+03	0.00E+00	+	**0.00E+00**	**0.00E+00**	=	**0.00E+00**	**0.00E+00**	=
4	**1.36E+01**	**0.00E+00**	7.03E+01	0.00E+00	+	1.37E+01	0.00E+00	+	**1.36E+01**	**0.00E+00**	=	1.37E+01	0.00E+00	+	**1.36E+01**	**0.00E+00**	=
5	**0.00E+00**	**0.00E+00**	**0.00E+00**	**0.00E+00**	=	5.71E-29	0.00E+00	+	6.56E-27	0.00E+00	+	**0.00E+00**	**0.00E+00**	=	9.57E-01	0.00E+00	+
6	**0.00E+00**	**0.00E+00**	1.80E+02	0.00E+00	=	4.29E+02	9.48E-03	+	4.92E+02	1.84E-03	+	2.24E+02	2.33E-01	+	5.02E+02	0.00E+00	+
7	**-8.42E+02**	**0.00E+00**	-7.01E+02	0.00E+00	+	-3.27E+02	9.38E-05	+	-2.77E+02	0.00E+00	+	-5.70E+01	0.00E+00	+	-8.94E+01	6.05E-04	+
8	**-2.84E-04**	**0.00E+00**	**-2.84E-04**	**0.00E+00**	=	**-2.84E-04**	**0.00E+00**	=	**-2.84E-04**	**0.00E+00**	=	**-2.84E-04**	**0.00E+00**	=	**-2.84E-04**	**0.00E+00**	=
9	**-2.67E-03**	**0.00E+00**	**-2.67E-03**	**0.00E+00**	=	**-2.67E-03**	**0.00E+00**	=	**-2.67E-03**	**0.00E+00**	=	-1.71E-04	1.69E-03	+	**-2.67E-03**	**0.00E+00**	=
10	**-1.03E-04**	**0.00E+00**	**-1.03E-04**	**0.00E+00**	=	**-1.03E-04**	**0.00E+00**	=	**-1.03E-04**	**0.00E+00**	=	**-1.03E-04**	**0.00E+00**	=	**-1.03E-04**	**0.00E+00**	=
11	**-2.65E+00**	**0.00E+00**	-9.25E-01	0.00E+00	+	-5.41E-01	5.71E-11	+	-7.69E+02	5.70E+01	+	-2.33E+03	9.48E+02	+	-2.82E+03	4.80E+03	+
12	**3.98E+00**	**0.00E+00**	4.61E+01	0.00E+00	+	**3.98E+00**	**0.00E+00**	=	3.99E+00	0.00E+00	+	7.28E+00	0.00E+00	+	**3.98E+00**	**0.00E+00**	=
13	**0.00E+00**	**0.00E+00**	2.89E-27	0.00E+00	+	3.54E+00	0.00E+00	+	5.16E+01	0.00E+00	+	**0.00E+00**	**0.00E+00**	=	**0.00E+00**	**0.00E+00**	=
14	**1.41E+00**	**0.00E+00**	1.63E+00	0.00E+00	+	**1.41E+00**	**0.00E+00**	=	**1.41E+00**	**0.00E+00**	=	2.03E+00	2.93E-01	+	**1.41E+00**	**0.00E+00**	=
15	**2.36E+00**	**0.00E+00**	6.75E+00	1.33E-02	+	5.87E+00	0.00E+00	+	5.00E+00	0.00E+00	+	2.34E+00	2.22E-06	+	5.25E+00	0.00E+00	+
16	**0.00E+00**	**0.00E+00**	**0.00E+00**	**0.00E+00**	=	1.57E+00	0.00E+00	+	6.28E+00	0.00E+00	+	**0.00E+00**	**0.00E+00**	=	6.28E+00	0.00E+00	+
17	**7.78E-01**	**1.45E+01**	9.72E-01	1.55E+01	+	1.83E-01	1.53E+01	+	8.73E-01	1.55E+01	+	5.28E-01	1.49E+01	+	7.21E-01	1.55E+01	+
18	**3.65E+01**	**0.00E+00**	3.66E+01	0.00E+00	=	1.81E+02	3.80E+03	+	**3.65E+01**	**0.00E+00**	=	1.12E+02	5.53E+02	+	3.22E+04	2.47E+09	+
19	9.79E-04	2.14E+04	7.60E+00	2.14E+04	+	**0.00E+00**	**2.14E+04**	-	**0.00E+00**	**2.14E+04**	-	-2.05E+01	2.14E+04	+	1.11E+02	2.14E+04	+
20	2.20E+00	0.00E+00	7.66E+00	0.00E+00	+	3.89E+00	0.00E+00	+	**1.93E+00**	**0.00E+00**	-	2.07E+00	0.00E+00	=	2.55E+00	0.00E+00	+
21	**1.07E+01**	**0.00E+00**	4.84E+01	0.00E+00	+	1.65E+01	0.00E+00	+	1.06E+01	0.00E+00	=	2.17E+02	2.73E+00	+	1.65E+01	0.00E+00	+
22	**0.00E+00**	**0.00E+00**	2.47E-25	0.00E+00	+	3.72E+01	0.00E+00	+	3.73E+03	0.00E+00	+	1.59E-01	0.00E+00	+	1.59E-01	0.00E+00	+
23	1.45E+00	0.00E+00	1.65E+00	0.00E+00	+	1.43E+00	0.00E+00	=	**1.41E+00**	**0.00E+00**	=	1.96E+00	0.00E+00	+	1.66E+00	0.00E+00	+
24	**2.36E+00**	**0.00E+00**	9.14E+00	0.00E+00	+	2.48E+00	0.00E+00	+	6.38E+00	0.00E+00	+	2.34E+00	9.27E-06	+	4.74E+00	0.00E+00	+
25	**0.00E+00**	**0.00E+00**	**0.00E+00**	**0.00E+00**	=	8.73E+00	0.00E+00	+	2.55E+01	0.00E+00	+	**0.00E+00**	**0.00E+00**	=	6.28E+00	0.00E+00	+
26	9.63E-01	1.55E+01	9.78E-01	1.55E+01	+	6.83E-01	1.55E+01	+	9.55E-01	1.55E+01	=	9.29E-01	1.55E+01	+	**7.87E-01**	**1.54E+01**	-
27	3.78E+01	0.00E+00	**3.66E+01**	**0.00E+00**	=	2.79E+02	6.57E+03	+	3.88E+01	0.00E+00	+	8.92E+01	1.32E+03	+	1.00E+05	2.27E+10	+
28	1.11E+02	2.15E+04	**5.84E+01**	**2.14E+04**	-	7.62E+01	2.15E+04	+	1.56E+02	2.15E+04	+	1.64E+01	2.14E+04	-	7.11E+01	2.14E+04	-
+/=/-				19/7/2			21/6/1			18/8/2			17/10/1			16/10/2	

Here first three algorithms are the top-ranked algorithm of IEEE CEC 2017's competition, and the last two are recently proposed algorithms.

In Tables. 3-6, the mean of the objective function and degree of constrained violation (denoted as "OF" and "CV") obtained from each algorithm over 25 independent runs for test problems with dimensions 10, 30, 50, and 100, respectively, are reported. In these tables, "−", "+" and "=" represent that performance of εDE-NGM is worse than, better than, and significantly equal to other algorithms, respectively, based on the Wilcoxon rank-sum test at 0.05 significance level.

In case of problems with dimension 10, the proposed algorithm performs edge over εMAgES, IUDE, εLSHADE44, CORCO, and DECODE on 19, 13, 14, 17, and 10 problems, respectively. However, other algorithms perform better than εDE-NGM on zero, three, three, zero, and four problems, respectively.

For problems with dimension 30, εDE-NGM is superior to other algorithms on 19, 21, 18, 17, and 16 problems, respectively, while other algorithms are better than two, one, two, one, and two problems, respectively.

As shown in Table. 5, the proposed algorithm performs better than other algorithms on 19, 21, 21, 16, and 19 problems

TABLE 5. Experimental outcomes of εDE-NGM and five selected contenders over 25 independent runs on the 28 test problems with dimension 50 from IEEE CEC 2017.

Prob	εDE-NGM OF	εDE-NGM CV	εMAg-ES OF	εMAg-ES CV	W	IUDE OF	IUDE CV	W	εLSHADE44 OF	εLSHADE44 CV	W	CORCO OF	CORCO CV	W	DECODE OF	DECODE CV	W
1	0.00E+00	0.00E+00	2.87E-27	0.00E+00	+	7.68E-28	0.00E+00	+	1.62E-24	0.00E+00	+	0.00E+00	0.00E+00	=	0.00E+00	0.00E+00	=
2	0.00E+00	0.00E+00	2.89E-27	0.00E+00	+	7.92E-28	0.00E+00	+	6.54E-25	0.00E+00	+	0.00E+00	0.00E+00	=	0.00E+00	0.00E+00	=
3	0.00E+00	0.00E+00	4.06E-27	0.00E+00	+	5.65E+02	0.00E+00	+	2.43E+04	0.00E+00	+	0.00E+00	0.00E+00	=	0.00E+00	0.00E+00	=
4	1.38E+01	0.00E+00	1.19E+02	0.00E+00	+	6.45E+01	0.00E+00	+	1.36E+01	0.00E+00	=	1.44E+01	0.00E+00	+	1.46E+01	0.00E+00	+
5	0.00E+00	0.00E+00	0.00E+00	0.00E+00	=	2.85E-28	0.00E+00	+	3.19E-01	0.00E+00	+	0.00E+00	0.00E+00	=	4.78E-01	0.00E+00	+
6	0.00E+00	0.00E+00	2.87E+02	0.00E+00	+	8.59E+02	1.61E-02	+	9.76E+02	9.38E-04	+	3.52E+02	1.20E-02	+	2.01E+03	2.74E-03	+
7	-1.21E+03	0.00E+00	-1.37E+03	0.00E+00	-	-1.96E+02	8.34E-05	+	-3.22E+02	0.00E+00	+	-3.88E+01	0.00E+00	+	-1.01E+02	6.68E-05	+
8	-1.34E-04	0.00E+00	-1.35E-04	0.00E+00	=	-1.33E-04	0.00E+00	=	-1.10E-04	0.00E+00	+	-1.32E-04	0.00E+00	=	-1.33E-04	0.00E+00	=
9	-2.04E-03	0.00E+00	6.66E-01	0.00E+00	+	-2.04E-03	0.00E+00	=	-1.74E-03	0.00E+00	+	-1.74E-03	0.00E+00	+	2.68E+00	1.68E-05	+
10	-4.82E-05	0.00E+00	-4.83E-05	0.00E+00	=	-4.83E-05	0.00E+00	=	-4.79E-05	0.00E+00	+	-4.81E-05	0.00E+00	+	-4.82E-05	0.00E+00	=
11	-2.86E+01	2.96E-02	-3.70E+00	2.26E-06	=	-1.21E+03	4.83E+01	+	-2.85E+03	1.09E+02	+	-3.99E+03	9.41E+02	+	-4.75E+03	4.96E+03	+
12	3.98E+00	0.00E+00	5.06E+01	0.00E+00	+	6.27E+00	0.00E+00	+	2.74E+01	0.00E+00	+	8.94E+00	0.00E+00	+	1.30E+01	0.00E+00	+
13	3.19E-01	0.00E+00	2.95E+02	0.00E+00	+	1.87E+01	0.00E+00	+	1.19E+01	0.00E+00	+	3.19E-01	0.00E+00	=	0.00E+00	0.00E+00	-
14	1.10E+00	0.00E+00	1.34E+00	0.00E+00	+	1.10E+00	0.00E+00	=	1.10E+00	0.00E+00	=	1.53E+00	0.00E+00	+	1.10E+00	0.00E+00	=
15	2.36E+00	0.00E+00	1.45E+01	2.05E-03	+	6.00E+00	0.00E+00	+	8.76E+00	0.00E+00	+	2.35E+00	0.00E+00	-	6.50E+00	0.00E+00	+
16	0.00E+00	0.00E+00	0.00E+00	0.00E+00	=	6.28E+00	0.00E+00	+	1.68E+01	0.00E+00	+	0.00E+00	0.00E+00	=	6.28E+00	0.00E+00	+
17	9.18E-01	2.46E+01	1.03E+00	2.55E+01	+	6.09E-01	2.54E+01	+	1.02E+00	2.55E+01	+	8.20E-01	2.53E+01	+	9.09E-01	2.55E+01	+
18	3.65E+01	0.00E+00	3.66E+01	0.00E+00	=	3.73E+02	1.17E+04	+	3.68E+01	0.00E+00	+	5.05E+02	3.33E+03	+	7.76E+04	8.29E+09	+
19	3.28E-01	3.61E+04	1.25E+01	3.61E+04	=	7.06E-01	3.61E+04	+	0.00E+00	3.61E+04	+	-3.57E+01	3.62E+04	+	1.68E-02	3.61E+04	+
20	3.97E+00	0.00E+00	1.52E+01	0.00E+00	+	8.68E+00	0.00E+00	+	3.50E+00	0.00E+00	-	3.72E+01	0.00E+00	=	4.12E+00	0.00E+00	+
21	1.23E+01	0.00E+00	5.53E+01	0.00E+00	+	1.13E+01	0.00E+00	+	1.14E+01	0.00E+00	+	4.04E+02	1.10E+01	+	2.59E+01	0.00E+00	+
22	4.30E+00	0.00E+00	9.76E+02	0.00E+00	+	4.63E+02	0.00E+00	+	1.26E+05	1.81E+01	+	1.15E+01	2.52E+00	+	2.02E+01	0.00E+00	+
23	1.11E+00	0.00E+00	1.34E+00	0.00E+00	+	1.10E+00	0.00E+00	=	1.10E+00	0.00E+00	=	1.51E+00	0.00E+00	+	1.53E+00	0.00E+00	+
24	2.36E+00	0.00E+00	1.22E+01	0.00E+00	+	4.24E+00	0.00E+00	+	9.27E+00	0.00E+00	+	2.35E+00	1.30E-06	+	5.37E+00	0.00E+00	+
25	0.00E+00	0.00E+00	0.00E+00	0.00E+00	=	7.60E+00	0.00E+00	+	7.89E+01	0.00E+00	+	0.00E+00	0.00E+00	=	6.28E+00	0.00E+00	+
26	1.03E+00	2.55E+01	1.03E+00	2.55E+01	+	9.18E-01	2.55E+01	=	1.03E+00	2.55E+01	=	9.69E-01	2.55E+01	+	1.01E+00	2.55E+01	=
27	3.83E+01	0.00E+00	3.65E+01	0.00E+00	=	4.95E+02	1.79E+04	+	4.03E+01	0.00E+00	+	5.43E+02	3.59E+03	+	2.51E+05	9.67E+10	+
28	2.18E+02	3.63E+04	9.53E+01	3.62E+04	-	1.82E+02	3.63E+04	=	2.79E+02	3.63E+04	+	5.60E+01	3.62E+04	-	1.79E+02	3.63E+04	-
+/=/-					19/5/4			21/7/0			21/4/3			16/10/2			19/7/2

TABLE 6. Experimental outcomes of εDE-NGM and five selected contenders over 25 independent runs on the 28 test problems with dimension 100 from IEEE CEC 2017.

Prob	εDE-NGM OF	εDE-NGM CV	εMAg-ES OF	εMAg-ES CV	W	IUDE OF	IUDE CV	W	εLSHADE44 OF	εLSHADE44 CV	W	CORCO OF	CORCO CV	W	DECODE OF	DECODE CV	W
1	0.00E+00	0.00E+00	3.98E-26	0.00E+00	+	1.31E-25	0.00E+00	+	1.90E-07	0.00E+00	+	0.00E+00	0.00E+00	=	0.00E+00	0.00E+00	=
2	0.00E+00	0.00E+00	3.98E-26	0.00E+00	+	8.19E-26	0.00E+00	+	1.03E-07	0.00E+00	+	0.00E+00	0.00E+00	=	0.00E+00	0.00E+00	=
3	0.00E+00	0.00E+00	4.43E-26	0.00E+00	+	3.34E+05	2.49E-06	+	1.66E+05	0.00E+00	+	0.00E+00	0.00E+00	=	0.00E+00	0.00E+00	=
4	4.52E+01	0.00E+00	2.51E+02	0.00E+00	+	2.84E+02	0.00E+00	+	1.44E+01	0.00E+00	-	6.06E+01	0.00E+00	+	8.19E+01	0.00E+00	+
5	0.00E+00	0.00E+00	2.69E+01	0.00E+00	+	6.39E+01	0.00E+00	+	4.40E+00	0.00E+00	+	5.24E+00	0.00E+00	+	1.45E+00	0.00E+00	+
6	2.88E+02	0.00E+00	8.06E+02	0.00E+00	+	4.04E+03	2.09E-02	+	3.00E+03	5.75E-04	+	7.05E+02	0.00E+00	+	2.27E+03	0.00E+00	+
7	-2.01E+03	0.00E+00	-2.48E+03	0.00E+00	-	-3.12E+02	4.36E-06	+	-4.77E+02	0.00E+00	+	-1.78E+02	0.00E+00	+	-8.04E+01	0.00E+00	+
8	-4.68E-05	0.00E+00	-4.55E-05	0.00E+00	+	8.33E-05	0.00E+00	+	1.68E-03	0.00E+00	+	1.85E-03	0.00E+00	+	1.01E+00	4.78E-05	+
9	9.18E-02	0.00E+00	3.04E+00	1.29E-02	+	3.33E-01	0.00E+00	+	4.18E-01	0.00E+00	+	2.79E-06	0.00E+00	-	0.00E+00	0.00E+00	-
10	-1.69E-05	0.00E+00	-1.16E-06	0.00E+00	+	3.68E-07	0.00E+00	+	1.53E-04	0.00E+00	+	4.79E-04	0.00E+00	+	1.63E-03	5.71E-05	+
11	-4.08E+03	6.23E+01	-6.67E+00	2.48E+01	-	-7.57E+03	4.67E-04	-	-7.41E+01	1.07E+02	+	-9.19E+03	1.44E+03	+	-9.75E+03	1.59E+04	+
12	5.66E+00	0.00E+00	3.01E+01	0.00E+00	+	1.47E+01	0.00E+00	+	1.88E+01	0.00E+00	+	1.08E+01	9.79E-01	+	1.98E+01	0.00E+00	+
13	5.53E+01	0.00E+00	4.14E+01	0.00E+00	-	1.91E+02	0.00E+00	+	6.79E+01	0.00E+00	+	2.48E+01	5.61E-01	+	4.25E+01	0.00E+00	=
14	7.85E-01	0.00E+00	9.58E-01	0.00E+00	+	7.88E-01	0.00E+00	+	8.36E-01	0.00E+00	+	1.12E+00	0.00E+00	+	8.57E-01	0.00E+00	+
15	2.36E+00	0.00E+00	8.64E+00	2.33E-04	+	1.56E+01	0.00E+00	+	1.62E+01	0.00E+00	+	1.39E+01	0.00E+00	+	1.23E+01	0.00E+00	+
16	0.00E+00	0.00E+00	0.00E+00	0.00E+00	=	9.44E+01	0.00E+00	+	1.88E+02	0.00E+00	+	0.00E+00	0.00E+00	=	6.28E+00	0.00E+00	+
17	1.04E+00	5.03E+01	1.09E+00	5.05E+01	+	1.06E+00	5.05E+01	+	1.10E+00	5.05E+01	+	1.00E+00	5.05E+01	+	1.08E+00	5.05E+01	+
18	3.64E+01	0.00E+00	3.64E+01	0.00E+00	=	5.89E+02	5.67E+04	+	3.79E+01	0.00E+00	+	1.08E+03	1.88E+04	+	1.89E+05	2.77E+10	+
19	2.18E+01	7.30E+04	8.99E+01	7.31E+04	+	8.65E+01	7.30E+04	-	0.00E+00	7.30E+04	=	-8.21E+01	7.31E+04	+	2.93E+02	7.30E+04	+
20	9.00E+00	0.00E+00	3.54E+01	0.00E+00	+	1.72E+01	0.00E+00	+	8.83E+00	0.00E+00	+	7.67E+00	0.00E+00	=	8.63E+00	0.00E+00	=
21	2.54E+01	0.00E+00	3.16E+01	0.00E+00	+	7.97E+00	0.00E+00	-	9.34E+00	0.00E+00	-	9.94E+02	1.04E+02	+	7.55E+00	0.00E+00	-
22	1.45E+02	0.00E+00	4.23E+03	0.00E+00	+	5.37E+04	7.48E+01	+	7.87E+05	1.33E+02	+	8.17E+02	1.02E+03	+	2.33E+02	0.00E+00	+
23	7.94E-01	0.00E+00	9.67E-01	0.00E+00	+	7.99E-01	0.00E+00	+	7.93E-01	0.00E+00	=	1.63E+00	8.66E+02	+	9.84E-01	0.00E+00	+
24	6.25E+00	0.00E+00	9.39E+00	0.00E+00	+	1.57E+01	0.00E+00	+	1.81E+01	0.00E+00	+	2.48E+00	0.00E+00	-	5.62E+00	0.00E+00	-
25	2.60E+01	0.00E+00	4.24E-14	0.00E+00	-	2.89E+02	0.00E+00	+	5.03E+02	0.00E+00	+	2.54E+01	0.00E+00	=	3.64E+01	0.00E+00	+
26	1.09E+00	5.05E+01	1.09E+00	5.05E+01	+	1.06E+00	5.05E+01	=	1.10E+00	5.05E+01	=	1.07E+00	5.05E+01	=	1.09E+00	5.05E+01	+
27	4.16E+01	0.00E+00	7.68E+01	8.65E-01	+	1.43E+03	3.09E+05	+	3.83E+02	6.50E+01	+	1.17E+03	2.64E+04	+	6.44E+05	3.31E+11	+
28	5.37E+02	7.34E+04	1.71E+02	7.31E+04	-	5.35E+02	7.34E+04	+	6.15E+02	7.34E+04	+	2.35E+02	7.33E+04	-	4.59E+02	7.33E+04	-
+/=/-					21/2/5			23/1/4			22/3/3			18/7/3			18/5/5

with dimension 50, respectively. On the other hand, other algorithms are superior on four, zero, three, two, and two problems, respectively.

In the case of problems with dimension 100, εDE-NGM outperforms other algorithms on 21, 23, 22, 18, and 18 test problems, respectively. In contrast, other algorithms' performance is better than εDE-NGM on five, four, three, three, and five test problems, respectively.

Following outcomes can be prepared from this comparative analysis.

1) Proposed algorithm determines a better optimum solution for most of the problems compared to others.

2) As compared to others, the proposed algorithm locates a feasible solution in each trial for most of the problems.

3) As compared to others, the proposed algorithm's performance does not deteriorate much with increasing dimensionality of the problem-space.

4) The proposed algorithm performs better than other algorithms in the case of COPs having a high number of equality constraints and a low volume of feasible regions.

Therefore, the above comparative analysis reveals that the proposed algorithm, εDE-NGM, is better than the

state-of-the-art algorithm on COPs, especially in the case of high dimension problems with more complex equality constraints.

B. EXPERIMENT 2: APPLICATION OF ϵDE-NGM ON POWER FLOW PROBLEMS

In this section, PF results are analyzed to validate the proposed algorithm (ϵDE-NGM) method. All PF algorithms reported in this paper are implemented in MATLAB R2018b environment in the computer with core i7, 3.2 GHz, and 8 GB of RAM. The initial start voltage is considered 1 p.u for all algorithms, and the termination of the algorithm is set as either based on tolerance or iteration. Four case studies were investigated to segregate the proposed algorithm (ϵDE-NGM) on different test systems viz. 6-bus, 33-bus, 69-bus, and 25-bus (unbalanced).

1) CASE I: 6-BUS MICROGRID

In this case, 6-bus test systems were adopted for the implementation of the proposed load flow algorithm. Fig. 2 shows the typical topology of the 6-bus test system. The load data and line connectivity data used in test systems are reported in ref. [69]. This system consists of three similar settings droop control of DGs on buses 4, 5, and 6 and operated in droop control mode. The detailed specifications such as location, active and reactive droop gain (np and mq), nominal frequency setpoint (ω^*), nominal voltage set point (V^*), and ratings of DGs S_{max}, Q_{max} are depicted in Table. 7.
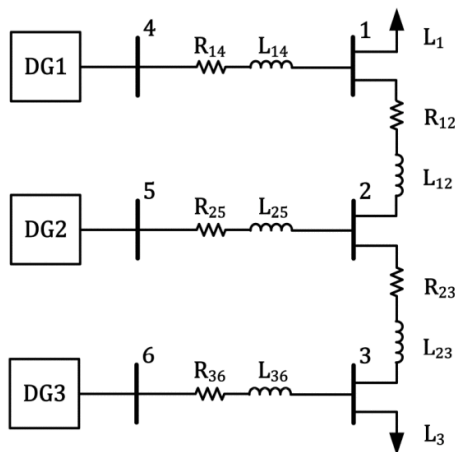
FIGURE 2. The 6-bus test system.

TABLE 7. Droop control settings of DGs in 6-Bus system.

DG	Location	np	nq	ω^*	V^*	S_{max}	Q_{max}
1	4	1.1439E-3	0.0591	1	1.01	1	0.7
2	5	1.1439E-3	0.0591	1	1.01	1	0.7
3	6	1.1439E-3	0.0591	1	1.01	1	0.7

To show the effectiveness of the proposed load flow algorithm (ϵDE-NGM) and a comparative analysis with the time

domain simulation modeled in PSCAD, evolutionary algorithms methods (GPSO-GM and ICGA) and deterministic method, i.e., NTR, are reported in Table. 8. The average magnitude and phase angle errors for the time-domain simulation model in PSCAD software are presented in Table. 9. From Table. 9, it is observed that the average phase and magnitude errors with the implementation of ϵDE-NGM method are lower as compared to the GPSO-GM, ICGA, and NTR method. More precisely, the average phase angle error in the case of ϵDE-NGM is 0.0126%, and the average magnitude error is 0.0189% w.r.t time domain simulation model. A small deviation in frequency is also observed while performing power flow by all algorithms. It is also important to note that the computational time required for ϵDE-NGM is lowest among all given algorithms.

As a summary, it is important to note that the PF result obtained from the proposed algorithm (ϵDE-NGM) shows good accuracy with respect to evolutionary algorithms methods (GPSO-GM and ICGA) and deterministic method (NTR).

2) CASE II: 33-BUS MICROGRID

A 33-bus distribution system with a rated voltage of 12.66 kV is used in this case study to demonstrate the proposed load flow algorithm. The single line diagram of the distribution system shown in Fig. 3 accommodating four DGs on bus numbers 26, 22, 25, and 9. The data related to line impedance and system load demand are adopted from [13].
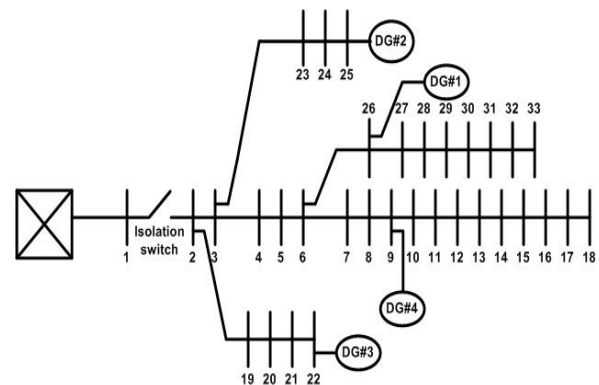

FIGURE 3. The 33-bus test system.

The detailed specifications such as location, active and reactive droop gain (np and mq), nominal frequency setpoint (ω^*), nominal voltage set point (V^*), and ratings of DGs S_{max}, Q_{max} are delineated in Table. 10. For a fair comparison, the power flow results obtained from ϵDE-GN is compared with existing evolutionary algorithms viz. GPSO-GM and ICGA.

In this case, all algorithms' performance has been evaluated after assuming all DGs have operated in droop control mode. The total active and reactive load demands on 33-bus islanded microgrid are 3.6790 MW and 2.2326 MVAr, respectively. In contrast, active and reactive power losses are 0.0428 MW and 0.0294 MVAr, respectively. The steady-state

TABLE 8. Power flow result of 6-Bus system test system.

Bus No.	Time domain model		ϵDE-NGM		GPSO-GM		ICGA		NTR	
	V (p.u)	δ (degree)	V (p.u)	δ (degree)	V (p.u)	δ (degree)	V (p.u)	δ (degree)	V (p.u)	δ (degree)
1	0.9605	0	0.9603	0	0.9608	0	0.9603	0	0.9601	0
2	0.9730	-5.2700	0.9726	-0.5257	0.9726	-0.5291	0.9728	-0.5282	0.9725	-0.5262
3	0.9643	-2.6850	0.9641	-2.6789	0.9647	-2.6837	0.9645	-2.6849	0.9638	-2.6822
4	0.9877	-0.0725	0.9873	-0.0729	0.9875	-0.0726	0.9874	-0.0726	0.9873	-0.0722
5	0.9906	-0.4520	0.9902	-0.4621	0.9903	-0.4516	0.9908	-0.4520	0.9901	-0.4510
6	0.9698	-2.8690	0.9692	-2.8644	0.9689	-2.8668	0.9700	-2.8691	0.9694	-2.8653
P_{loss}	0.0080		0.0080		0.0080		0.0090		0.0090	
Frequency	0.99908		0.99908		0.99924		0.99922		0.99924	
Run time	0.0510		0.0072		0.0097		0.0092		0.0220	

TABLE 9. Average error with respect to Time simulation model.

Error (%)	ϵDE-NGM	GPSO-GM	ICGA	NTR
Magnitude	**0.0189**	0.0428	0.0222	0.0461
Phase	**0.0126**	0.1250	0.0273	0.1696

TABLE 10. Droop control settings of DGs in 33-Bus system.

DG	Location	np	mq	ω^*	V^*	S_{max}	Q_{max}
1	26	0.705E-3	0.01667	1	1.02	3.00	1.80
2	22	2.252E-3	0.05000	1	1.02	1.00	0.60
3	25	4.504E-3	0.01000	1	1.02	0.50	0.30
4	9	3.003E-3	0.06670	1	1.02	0.75	0.45
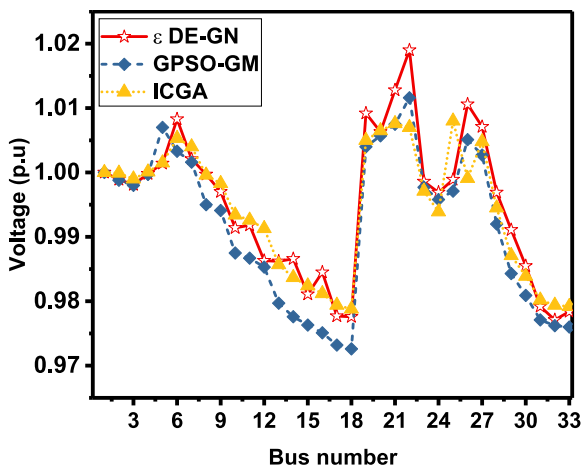
FIGURE 4. Bus-wise voltage of 33-bus islanded microgrid.

FIGURE 5. Bus-wise angle of 33-bus islanded microgrid.
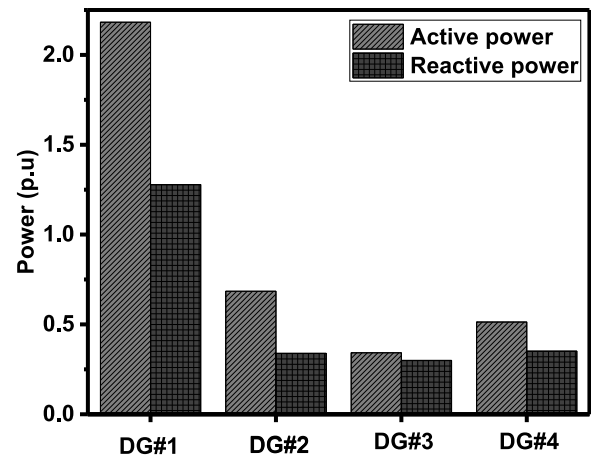
FIGURE 6. Active and reactive power sharing of DGs on the 33 bus islanded microgrid.

frequency obtained by ϵDE-NGM for this case is 0.99845 p.u. The voltage magnitude and phase angle obtained from all algorithms are compared in Figs. 4 and 5. Fig. 4 shows that the average magnitude of ϵDE-NGM with respect to GPSO-GM and ICGA is 0.338% and 0.276%, respectively. Whereas, Fig. 5, it is observed that the average phase angle error of ϵDE-NGM with respect to GPSO-GM and ICGA is 0.419% and 0.105%, respectively.

The active and reactive power sharing by individual DGs are shown in Fig. 6. It is observed that reactive power-sharing of DG#2 and DG# 3 has reached its maximum capacity whereas, other DGs shares within their limits. It is also observed that all DGs are operated within permissible

apparent power rating. The statistical index parameter such as standard deviation (SD), worst value (WV), and Best mean (BM) obtained after 55 runs for all evolutionary algorithms are compared in Table. 11. From Table. 11, it can be concluded that the proposed algorithm (ϵDE-NGM) requires less run time and lower SD, WV, and BM among all evolutionary algorithms.

TABLE 11. Statistical parameters for 33-bus microgrid.

Algorithm	Statistical Parameter			Average time (Sec.)
	SD	WV	BM	
ϵDE-NGM	2.47E-6	1.02E-7	8.71E-8	1.16
GPSO-GM	1.25E-7	1.00E-7	8.62E-8	1.40
ICGA	1.25E-7	1.06E-7	8.62E-8	1.40
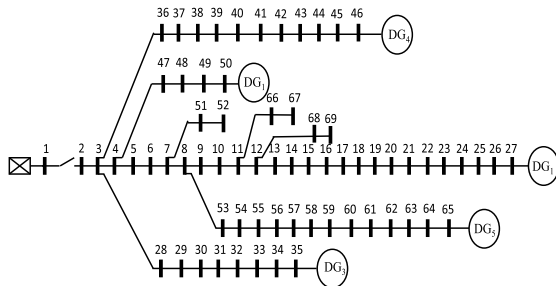
FIGURE 7. Topology of 69-Bus system.

TABLE 12. Droop control settings of DGs in 69-Bus system.

DG	Location	np	mq	ω^*	V^*	S_{max}	Q_{max}
1	50	1.501E-3	0.03333	1	1.04	1.5	0.9
2	27	4.504E-3	0.01000	1	1.04	0.5	0.3
3	35	2.308E-3	0.05000	1	1.04	1.0	0.6
4	46	2.308E-3	0.05000	1	1.04	1.0	0.6
5	55	1.501E-3	0.03333	1	1.04	1.5	0.9

3) CASE III: 69-BUS MICROGRID

The IEEE 69 bus distribution system shown in Fig.7 has been considered for this case study. This system is having with total active and reactive loads of 3.772 MW and 2.694 MVAr, respectively. Bus number 50, 27, 35, 46, and 65 are considered for DGs installation. The data related to line impedance and system load demand are taken from ref. [13].

The detailed specifications such as location, active and reactive droop gain (np and mq), nominal frequency setpoint (ω^*), nominal voltage set point (V^*), and ratings of DGs S_{max}, Q_{max} are delineated in Table.12. For a fair comparison, the power flow results obtained from ϵDE-NGM is compared with existing evolutionary algorithms viz. GPSO-GM and ICGA.

In this case, all algorithms' performance has been evaluated after assuming all DGs have operated in droop control mode. The total active power and reactive power load demand on the distribution system are 3.7722 MW and 2.6941 MVAR, respectively, whereas active and reactive power losses are 0.0868 MW and 0.0424 MVAr. The steady-state frequency obtained by ϵDE-NGM is 0.9983 p.u. The voltage magnitude and phase angle obtained from all algorithms are compared in Figs. 8 and 9. From Fig. 8, it is observed that the average magnitude of ϵDE-NGM with respect to evolutionary algorithms (GPSO-GM and ICGA) is 0.253%. Whereas, Fig. 9, it is observed that the average phase angle error of ϵDE-NGM with respect to evolutionary algorithms (GPSO-GM and ICGA) is 0.112%.
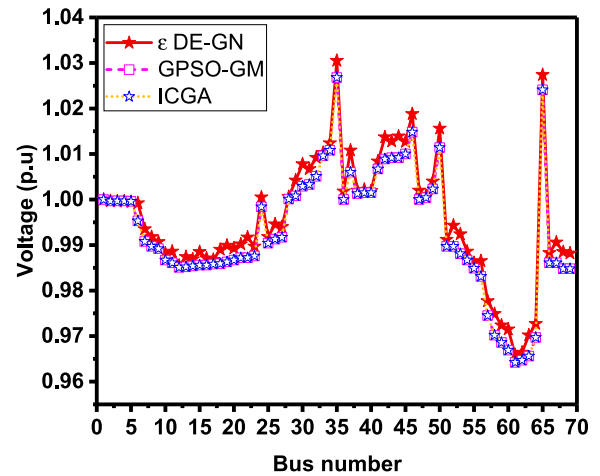
FIGURE 8. Bus-wise volatge of 69-bus islanded microgrid.
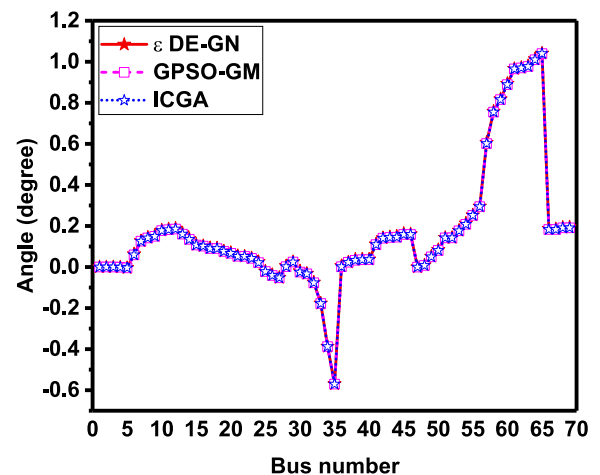
FIGURE 9. Bus-wise angle of 69-bus islanded microgrid.

TABLE 13. Statistical parameters for 69-bus microgrid.

Algorithm	Statistical Parameter			Average time (Sec.)
	SD	WV	BM	
ϵDE-NGM	1.47E-6	2.60E-7	6.54E-8	1.28
GPSO-GM	4.61E-7	1.31E-7	8.62E-8	1.51
ICGA	4.61E-7	1.31E-7	8.62E-8	1.51

The active and reactive power sharing by individual DGs are shown in Fig. 10. It is observed that reactive power-sharing of DG#1, DG#2, and DG# 3 has reached its maximum capacity whereas, other DGs shares within their limits. It is also observed that all DGs are operated within permissible apparent power rating. The statistical index parameter such as standard deviation (SD), worst value (WV), and Best mean (BM) obtained after 55 runs for all evolutionary algorithms are compared in Table. 13. From Table. 13, it can be concluded that the proposed algorithm (ϵDE-NGM) requires less run time and lower SD, WV, and BM among all evolutionary algorithms.
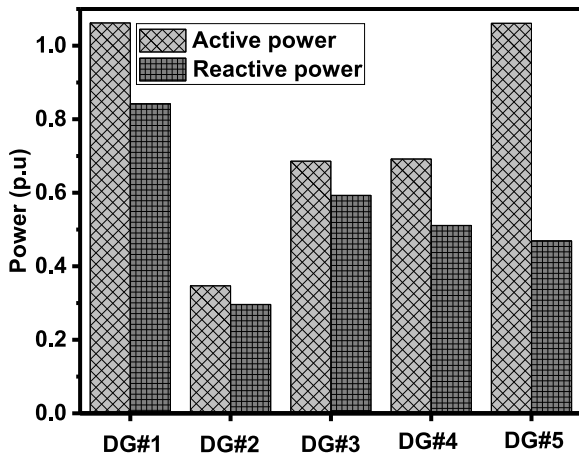
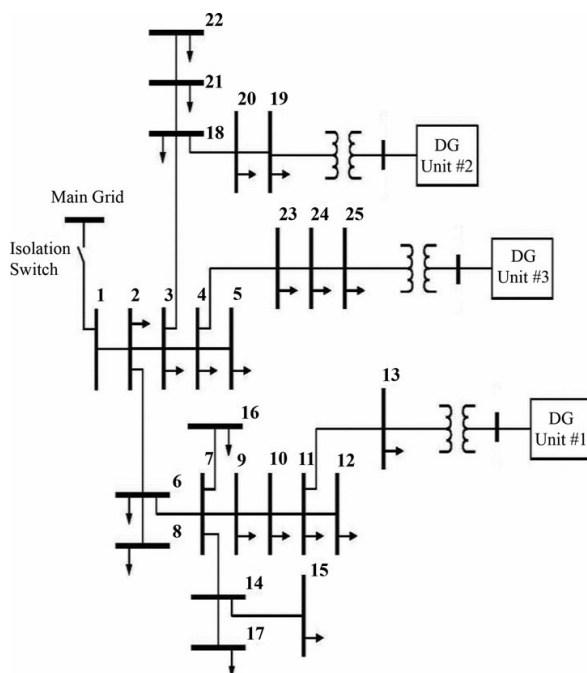**FIGURE 10.** Active and reactive power sharing of DGs on the 69 bus islanded microgrid.

FIGURE 11. Topology of 25-Bus unbalanced microgrid.

4) CASE IV: 25-BUS UNBALANCED MICROGRID

The 25-bus unbalanced microgrid with the rated voltage of 12.66 kV has been adopted for this study. The single line diagram of the distribution system is shown in Fig. 11. The load data, line connectivity, and impedance for a different type of conductor used in the distribution system are given in [69]. Three DGs were installed at bus number 13, 19, and 25. It is assumed that all the DGs are operated in a balanced condition.

The detailed specifications such as location, active and reactive power gain (np and mq), nominal frequency setpoint (ω^*), nominal voltage set point (V^*), and ratings of DGs S_{max}, Q_{max} are delineated in Table. 14.

TABLE 14. Droop control settings of DGs in 25-Bus system.

DG	Location	np	mq	ω^*	V^*	S_{max}	Q_{max}
1	13	0.005	0.05	1	1.01	0.6	0.360
2	19	0.010	0.10	1	1.01	0.3	0.180
3	25	0.005	0.05	1	1.01	0.6	0.194

TABLE 15. Statistical parameters for 25-bus unbalanced microgrid.

Algorithm	Statistical Parameter			Average time (Sec.)
	SD	WV	BM	
ϵDE-NGM	2.13E-5	1.70E-6	4.49E-8	1.102
GPSO-GM	3.23E-6	4.27E-6	4.49E-7	1.378
ICGA	4.61E-7	1.31E-7	8.62E-8	1.378

The steady-state frequency obtained by the proposed algorithm (ϵDE-NGM) is 0.99812. Total active and reactive power losses are 0.0196 and 0.0143 p.u, respectively. Fig. 12 shows the comparison of the bus-wise voltage profile for all three phases. The maximum average voltage magnitude error of ϵDE-NGM concerning evolutionary algorithms (GPSO-GM and ICGA) is 0.164% at bus number 22 of phase-A. Whereas the maximum average voltage angle error of ϵDE-NGM concerning evolutionary algorithms (GPSO-GM and ICGA) is 0.21% at bus number 22 of phase-B. The active and reactive power sharing of all individual DGs based on their individual specification and setting are shown in Figs. 14 and 15. From Fig. 15, it is observed that DG#1 and DG#2 are operated at maximum reactive power capacity. Whereas, only DG#3 is operated at lower to its maximum capacity and operated in droop controlled mode. It is also important to note that DGs' apparent power-sharing is also within the specified limit. The statistical index parameter such as standard deviation (SD), worst value (WV), and best mean (BM) obtained after 55 runs for all evolutionary algorithms are compared in Table. 15. From Table. 15, it can be concluded that the proposed algorithm (ϵDE-NGM) requires less run time and lower SD, WV, and BM among all evolutionary algorithms.

As a summary, ϵDE-NGM methods are well performed in all cases. In case I: 6-bus system, the proposed algorithm is compared to time-domain simulation modeled in PSCAD, evolutionary algorithms methods (GPSO-GM and ICGA), and deterministic method, i.e., NTR. the power flow result obtained from the proposed algorithm (ϵDE-NGM) shows good accuracy with respect to evolutionary algorithms methods (GPSO-GM and ICGA) and deterministic method (NTR).

In Case II and Case III, the 33-bus and 69-bus balanced microgrid are adopted for analyses purpose. Whereas, In Case-IV, the 25-bus unbalanced microgrid system is considered for the study. For a fair comparison, power flow results obtained from the proposed algorithm (ϵDE-NGM) is compared with GPSO-GM and ICGA algorithm.

C. ROBUST ANALYSIS

In this section, the proposed algorithm's robustness is analyzed on several hard-to-solve ill-conditioned and unsolvable
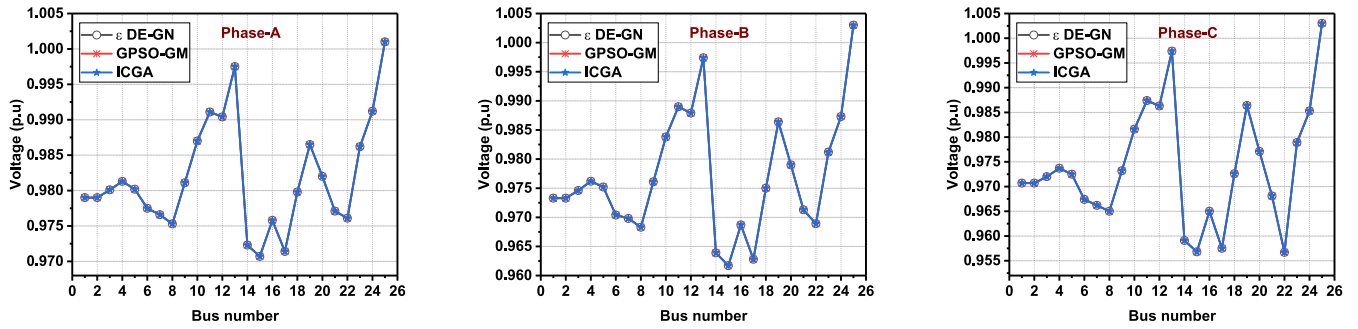
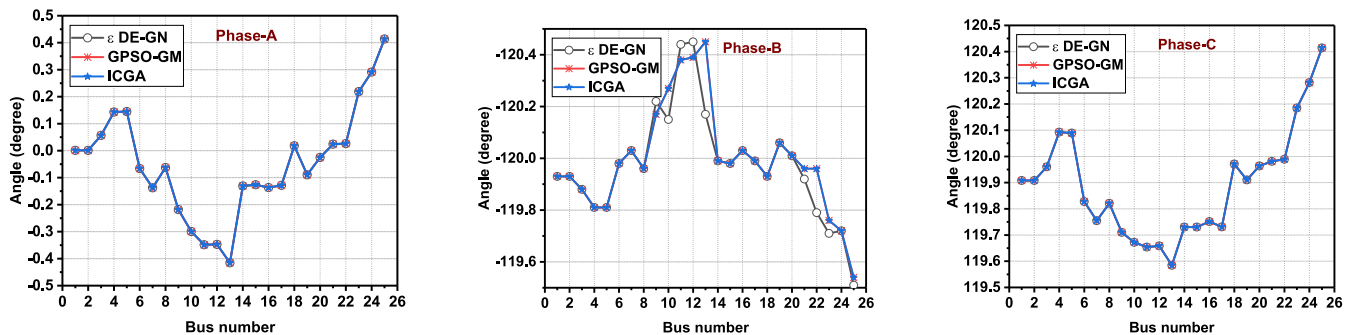**FIGURE 12.** Phase-wise bus voltage of 25-bus microgrid.

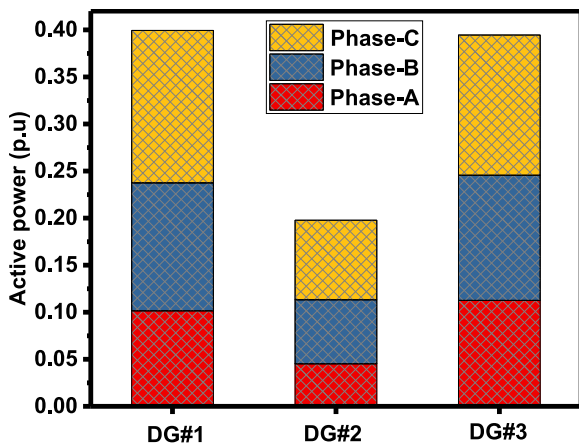**FIGURE 13.** Phase-wise bus angle of 25-bus microgrid.

FIGURE 14. Active power sharing of individual DGs on 25-bus microgrid.
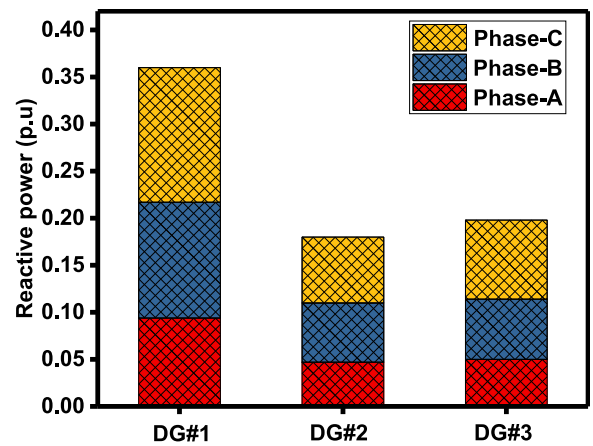

FIGURE 15. Reactive power sharing of individual DGs on 25-bus microgrid.

test problems. Here, unbalanced microgrids are considered for this experiment. System data of all these test systems are available online in https://github.com/abhisheka456/Test-Systems. The performance of the proposed algorithm is compared with the following state-of-the-art algorithms' performance:

1) Newton-Trust region (NTR) algorithm [11],
2) Projected Levenberg-Marquardt (PLM) algorithm [25],
3) Implicit Z-bus (IZBUS) algorithm [36], and
4) Guaranteed convergence particle swarm optimization with Gaussian mutation (GPSO-GM) [20].

Two stopping criteria are considered to terminate all above-mentioned algorithms, including proposed algorithms:

i) convergence tolerance is 10^{-6} pu, and
ii) maximum allowed computation time is 2 hours.

As shown in the Table 16, two classes of ill-conditioned test systems are considered. In the first case, heavily loaded systems are considered, while systems with faulty lines are selected for the second case of the ill-conditioned systems. In all test systems, the proposed algorithm can provide an operating power flow solution effectively. As compared to

TABLE 16. Comparison of computation time required by different algorithms. (NC: Not Converged).

System	NTR	PLM	IZBUS	GPSO-GM	ϵDE-NGM
Ill-conditioned Test Systems					
Case180	118.3	121.8	NC	NC	**78.8**
Case205	133.8	NC	NC	NC	**101.3**
Case375	400.3	NC	NC	NC	**360.2**
Case505	NC	NC	NC	NC	**730.4**
Case805	NC	NC	NC	NC	**823.8**
Ill-conditioned due to faulty lines					
Case25	2.6	2.3	NC	NC	**1.2**
Case35	13.2	NC	NC	NC	**10.1**
Case59	25.4	NC	NC	NC	**13.3**
Case123	33.2	68.2	NC	NC	**21.6**

other existing algorithms, the proposed algorithm performs better than other ones in the case of all ill-conditioned test systems considered here.

This experiment's overall analysis suggests that the proposed algorithm can solve ill-conditioned test systems more robustly than other algorithms.

VI. CONCLUSION

In this paper, a globally convergent algorithm based on DE is proposed for the PF problem of DCIMGs. The operating frequency is described as an additional PF variable in the proposed method. DGs' operations are modeled in droop, PV, and PQ modes as per the DCIMGs' characteristics. Then, the proposed PF problem is transformed into a COP that can be solved using optimization algorithms. For solving COPs, a DE-based algorithm, named ϵDE-NGM, is proposed by incorporating the NGM operator in the DE framework. The performance of the proposed algorithm is verified on the benchmark problems. The outcomes reveal that it performs better than existing algorithms in terms of the solution's quality and convergence in COPs with high number of equality constraints. After that, the proposed algorithm is applied to a balanced and unbalanced DCIMG to analyze its performance. The proposed algorithms' performance is compared with the time-domain simulation modeled in PSCAD, evolutionary algorithms methods (GPSO-GM and ICGA), and conventional method, i.e., NTR. The obtained results reveal that the performance of the proposed algorithm is superior to others. The main contributions of this work can be summarized as follows.

1) In this paper, the PF problem of a DCIMGS is transformed into COPs to develop a global-convergent PF analysis tool using optimization algorithms.

2) A metaheuristic, named as ϵDE-NGM, is proposed to solve COPs with a high number of equality constraints effectively. Further, this algorithm is applied to the PF problem of DCIMGs.

3) The performance of the proposed algorithm is analyzed on modern benchmark problems. The obtained performance is compared with the state-of-the-art algorithms. Experimental results show that the proposed algorithm

is more effective than other algorithms over COPs having a good number of equality constraints.

4) At last, the proposed algorithm is tested on the different types of test problems. Obtained outcomes suggest that the proposed algorithm performs very well on different problems, especially ill-conditioned and unsolvable test cases concerning other algorithms.

Overall, the proposed technique provides robust and effective performance in terms of convergence and efficiency. Consequently, it is suggested to further implement this algorithm to probabilistic PF analysis of DCIMGs in the future.

REFERENCES

[1] H. Wu, X. Liu, and M. Ding, "Dynamic economic dispatch of a microgrid: Mathematical models and solution algorithm," *Int. J. Electr. Power Energy Syst.*, vol. 63, pp. 336–346, Dec. 2014.

[2] M. H. Moradi, M. Abedini, and S. M. Hosseinian, "Improving operation constraints of microgrid using PHEVs and renewable energy sources," *Renew. Energy*, vol. 83, pp. 543–552, Nov. 2015.

[3] T. C. Green and M. Prodanović, "Control of inverter-based micro-grids," *Electr. Power Syst. Res.*, vol. 77, no. 9, pp. 1204–1213, Jul. 2007.

[4] T. L. Vandoorn, B. Meersman, J. D. M. De Kooning, and L. Vandevelde, "Analogy between conventional grid control and islanded microgrid control based on a global DC-link voltage droop," *IEEE Trans. Power Del.*, vol. 27, no. 3, pp. 1405–1414, Jul. 2012.

[5] F. Gao and M. R. Iravani, "A control strategy for a distributed generation unit in grid-connected and autonomous modes of operation," *IEEE Trans. Power Del.*, vol. 23, no. 2, pp. 850–859, Apr. 2008.

[6] C. S. Cheng and D. Shirmohammadi, "A three-phase power flow method for real-time distribution system analysis," *IEEE Trans. Power Syst.*, vol. 10, no. 2, pp. 671–679, May 1995.

[7] M. Abdel-Akher, K. M. Nor, and A. H. A. Rashid, "Improved three-phase power-flow methods using sequence components," *IEEE Trans. Power Syst.*, vol. 20, no. 3, pp. 1389–1397, Aug. 2005.

[8] M. Abedini, M. H. Moradi, and S. M. Hosseinian, "Optimal clustering of MGs based on droop controller for improving reliability using a hybrid of harmony search and genetic algorithms," *ISA Trans.*, vol. 61, pp. 119–128, Mar. 2016.

[9] V. M. da Costa, M. L. de Oliveira, and M. R. Guedes, "Developments in the analysis of unbalanced three-phase power flow solutions," *Int. J. Electr. Power Energy Syst.*, vol. 29, no. 2, pp. 175–182, Feb. 2007.

[10] D. Mendive, *An Application of Ladder Network Theory to the Solution of Three-Phase Radial Load-Flow Problems*. Las Cruces, NM, USA: New Mexico State Univ., 1975. [Online]. Available: https://books.google.co.in/books?id=akFPGwAACAAJ

[11] M. M. A. Abdelaziz, H. E. Farag, E. F. El-Saadany, and Y. A.-R.-I. Mohamed, "A novel and generalized three-phase power flow algorithm for islanded microgrids using a Newton trust region method," *IEEE Trans. Power Syst.*, vol. 28, no. 1, pp. 190–201, Feb. 2013.

[12] A. M. Vural, "Interior point-based slack-bus free-power flow solution for balanced islanded microgrids," *Int. Trans. Electr. Energy Syst.*, vol. 26, no. 5, pp. 968–992, May 2016.

[13] G. Diaz, J. Gomez-Aleixandre, and J. Coto, "Direct backward/forward sweep algorithm for solving load power flows in AC droop-regulated microgrids," *IEEE Trans. Smart Grid*, vol. 7, no. 5, pp. 2208–2217, Sep. 2016.

[14] A. Kumar, B. K. Jha, D. K. Dheer, D. Singh, and R. K. Misra, "Nested backward/forward sweep algorithm for power flow analysis of droop regulated islanded microgrids," *IET Gener., Transmiss. Distrib.*, vol. 13, no. 14, pp. 3086–3095, Jul. 2019.

[15] F. Mumtaz, M. H. Syed, M. A. Hosani, and H. H. Zeineldin, "A simple and accurate approach to solve the power flow for balanced islanded microgrids," in *Proc. IEEE 15th Int. Conf. Environ. Electr. Eng. (EEEIC)*, Jun. 2015, pp. 1852–1856.

[16] F. Mumtaz, M. H. Syed, M. A. Hosani, and H. H. Zeineldin, "A novel approach to solve power flow for islanded microgrids using modified Newton–Raphson with droop control of DG," *IEEE Trans. Sustain. Energy*, vol. 7, no. 2, pp. 493–503, Apr. 2016.

[17] A. Kumar, B. K. Jha, D. K. Dheer, R. K. Misra, and D. Singh, "A nested-iterative Newton–Raphson based power flow formulation for droop-based islanded microgrids," *Electr. Power Syst. Res.*, vol. 180, Mar. 2020, Art. no. 106131.

[18] A. Kumar, B. K. Jha, D. Singh, and R. K. Misra, "Current injection-based Newton–Raphson power-flow algorithm for droop-based islanded microgrids," *IET Gener., Transmiss. Distrib.*, vol. 13, no. 23, pp. 5271–5283, Dec. 2019.

[19] A. Elrayyah, Y. Sozer, and M. E. Elbuluk, "A novel load-flow analysis for stable and optimized microgrid operation," *IEEE Trans. Power Del.*, vol. 29, no. 4, pp. 1709–1717, Aug. 2014.

[20] A. Esmaeli, M. Abedini, and M. H. Moradi, "A novel power flow analysis in an islanded renewable microgrid," *Renew. Energy*, vol. 96, pp. 914–927, Oct. 2016.

[21] K. P. Wong, A. Li, and M. Law, "Development of constrained-genetic-algorithm load-flow method," *IEE Proc.-Gener., Transmiss. Distrib.*, vol. 144, no. 2, pp. 91–99, 1997.

[22] K. P. Wong, A. Li, and T. Law, "Advanced, constrained, genetic algorithm load flow method," *IEE Proc.-Gener., Transmiss. Distrib.*, vol. 146, no. 6, pp. 609–616, 1999.

[23] M. Abedini, "A novel algorithm for load flow analysis in island microgrids using an improved evolutionary algorithm," *Int. Trans. Electr. Energy Syst.*, vol. 26, no. 12, pp. 2727–2743, Dec. 2016.

[24] M. H. Moradi, V. B. Foroutan, and M. Abedini, "Power flow analysis in islanded micro-grids via modeling different operational modes of DGs: A review and a new approach," *Renew. Sustain. Energy Rev.*, vol. 69, pp. 248–262, Mar. 2017.

[25] Y. Ju, J. Wang, Z. Zhang, Y. Huang, and Y. Lin, "A calculation method for three-phase power flow in micro-grid based on smooth function," *IEEE Trans. Power Syst.*, vol. 35, no. 6, pp. 4896–4903, Nov. 2020.

[26] A. Kumar, S. Das, R. K. Misra, and D. Singh, "A v-constrained matrix adaptation evolution strategy with broyden-based mutation for constrained optimization," *IEEE Trans. Cybern.*, early access, Feb. 26, 2021, doi: 10.1109/TCYB.2020.3042853.

[27] M. A. Allam, A. A. Hamad, and M. Kazerani, "A generic modeling and power-flow analysis approach for isochronous and droop-controlled microgrids," *IEEE Trans. Power Syst.*, vol. 33, no. 5, pp. 5657–5670, Sep. 2018.

[28] N. Cai and A. R. Khatib, "A universal power flow algorithm for industrial systems and microgrids—Active power," *IEEE Trans. Power Syst.*, vol. 34, no. 6, pp. 4900–4909, Nov. 2019.

[29] A. A. Nazari, R. Keypour, M. H. Beiranvand, and N. Amjady, "A decoupled extended power flow analysis based on Newton–Raphson method for islanded microgrids," *Int. J. Electr. Power Energy Syst.*, vol. 117, May 2020, Art. no. 105705.

[30] Z. Pan, J. Wu, T. Ding, J. Liu, F. Wang, and X. Tong, "Load flow calculation for droop-controlled islanded microgrids based on direct Newton–Raphson method with step size optimisation," *IET Gener., Transmiss. Distrib.*, vol. 14, no. 21, pp. 4775–4787, Nov. 2020.

[31] A. Kumar, S. Das, and R. Mallipeddi, "An inversion-free robust power flow algorithm for microgrids," *IEEE Trans. Smart Grid*, early access, Mar. 8, 2021, doi: 10.1109/TSG.2021.3064656.

[32] F. Hameed, M. Al Hosani, and H. H. Zeineldin, "A modified backward/forward sweep load flow method for islanded radial microgrids," *IEEE Trans. Smart Grid*, vol. 10, no. 1, pp. 910–918, Jan. 2019.

[33] M. E. Nassar and M. M. A. Salama, "A novel branch-based power flow algorithm for islanded AC microgrids," *Electr. Power Syst. Res.*, vol. 146, pp. 51–62, May 2017.

[34] D. Manna, S. K. Goswami, and P. K. Chattopadhyay, "A power flow solution technique for autonomous and non autonomous mode of operation of microgrid system," *Electr. Power Compon. Syst.*, vol. 46, no. 4, pp. 429–444, Feb. 2018.

[35] L. Ren and P. Zhang, "Generalized microgrid power flow," *IEEE Trans. Smart Grid*, vol. 9, no. 4, pp. 3911–3913, Jul. 2018.

[36] E. E. Pompodakis, G. C. Kryonidis, and M. C. Alexiadis, "A comprehensive load flow approach for grid-connected and islanded AC microgrids," *IEEE Trans. Power Syst.*, vol. 35, no. 2, pp. 1143–1155, Mar. 2020.

[37] R. Raj and P. S. Babu, "A backward/forward method for solving load flows in droop-controlled microgrids," in *Control Applications in Modern Power System*. Singapore: Springer, 2021, pp. 367–377.

[38] Y. Vilaisarn and M. Abdelaziz, "An inversion-free sparse Z power flow algorithm for large-scale droop controlled islanded microgrids," *Int. J. Electr. Power Energy Syst.*, vol. 121, Oct. 2020, Art. no. 106048.

[39] N. Pogaku, M. Prodanovic, and T. C. Green, "Modeling, analysis and testing of autonomous operation of an inverter-based microgrid," *IEEE Trans. Power Electron.*, vol. 22, no. 2, pp. 613–625, Mar. 2007.

[40] R. Storn and K. Price, "Differential evolution—A simple and efficient heuristic for global optimization over continuous spaces," *J. Global Optim.*, vol. 11, no. 4, pp. 341–359, 1997.

[41] R. Mallipeddi and P. N. Suganthan, "Ensemble of constraint handling techniques," *IEEE Trans. Evol. Comput.*, vol. 14, no. 4, pp. 561–579, Aug. 2010.

[42] J. Liang, B. Qu, and P. Suganthan, "Problem definitions and evaluation criteria for the CEC 2014 special session and competition on single objective real-parameter numerical optimization," Comput. Intell. Lab., Zhengzhou Univ., Zhengzhou, China, Nanyang Technol. Univ., Singapore, Tech. Rep. 201311, 2013.

[43] N. Awad, M. Ali, J. Liang, B. Qu, and P. Suganthan, "Problem definitions and evaluation criteria for the CEC 2017 special session and competition on single objective real-parameter numerical optimization," Tech. Rep., 2016.

[44] E. Mezura-Montes, J. Velazquez-Reyes, and C. A. C. Coello, "Modified differential evolution for constrained optimization," in *Proc. IEEE Int. Conf. Evol. Comput.*, Jul. 2006, pp. 25–32.

[45] K. Deb, "An efficient constraint handling method for genetic algorithms," *Comput. Methods Appl. Mech. Eng.*, vol. 186, nos. 2–4, pp. 311–338, Jun. 2000.

[46] S. M. Elsayed, R. A. Sarker, and D. L. Essam, "Multi-operator based evolutionary algorithms for solving constrained optimization problems," *Comput. Oper. Res.*, vol. 38, no. 12, pp. 1877–1896, Dec. 2011.

[47] S. M. Elsayed, R. A. Sarker, and D. L. Essam, "An improved self-adaptive differential evolution algorithm for optimization problems," *IEEE Trans. Ind. Informat.*, vol. 9, no. 1, pp. 89–99, Feb. 2013.

[48] S. M. Elsayed, R. A. Sarker, and D. L. Essam, "A self-adaptive combined strategies algorithm for constrained optimization using differential evolution," *Appl. Math. Comput.*, vol. 241, pp. 267–282, Aug. 2014.

[49] B.-C. Wang, H.-X. Li, J.-P. Li, and Y. Wang, "Composite differential evolution for constrained evolutionary optimization," *IEEE Trans. Syst., Man, Cybern. Syst.*, vol. 49, no. 7, pp. 1482–1495, Jul. 2018.

[50] Y. Lu, J. Zhou, H. Qin, Y. Li, and Y. Zhang, "An adaptive hybrid differential evolution algorithm for dynamic economic dispatch with valve-point effects," *Expert Syst. Appl.*, vol. 37, no. 7, pp. 4842–4849, Jul. 2010.

[51] W.-F. Gao, G. G. Yen, and S.-Y. Liu, "A dual-population differential evolution with coevolution for constrained optimization," *IEEE Trans. Cybern.*, vol. 45, no. 5, pp. 1108–1121, May 2015.

[52] X. Yu, Y. Lu, X. Wang, X. Luo, and M. Cai, "An effective improved differential evolution algorithm to solve constrained optimization problems," *Soft Comput.*, vol. 23, no. 7, pp. 2409–2427, Apr. 2019.

[53] A. Trivedi, K. Sanyal, P. Verma, and D. Srinivasan, "A unified differential evolution algorithm for constrained optimization problems," in *Proc. IEEE Congr. Evol. Comput. (CEC)*, Jun. 2017, pp. 1231–1238.

[54] A. Trivedi, K. Sanyal, P. Verma, and D. Srinivasan, "A unified differential evolution algorithm for constrained optimization problems," in *Proc. IEEE Congr. Evol. Comput. (CEC)*, Jun. 2017, pp. 1–10.

[55] S. Das, S. S. Mullick, and P. N. Suganthan, "Recent advances in differential evolution—An updated survey," *Swarm Evol. Comput.*, vol. 27, pp. 1–30, Apr. 2016.

[56] A. Kumar, S. Das, and R. Mallipeddi, "A reference vector-based simplified covariance matrix adaptation evolution strategy for constrained global optimization," *IEEE Trans. Cybern.*, early access, Sep. 16, 2020, doi: 10.1109/TCYB.2020.3013950.

[57] A. Kumar, G. Wu, M. Z. Ali, R. Mallipeddi, P. N. Suganthan, and S. Das, "A test-suite of non-convex constrained optimization problems from the real-world and some baseline results," *Swarm Evol. Comput.*, vol. 56, Aug. 2020, Art. no. 100693.

[58] J. E. Dennis, D. M. Gay, and R. E. Welsch, "An adaptive nonlinear least square algorithm," Cornell Univ., Ithaca, NY, USA, Tech. Rep. TR77-321, 1977.

[59] T. Takahama and S. Sakai, "Constrained optimization by ε constrained particle swarm optimizer with ε-level control," in *Soft Computing as Transdisciplinary Science and Technology*. Berlin, Germany: Springer, 2005, pp. 1019–1029.

[60] Z. Hu, S. Xiong, Q. Su, and X. Zhang, "Sufficient conditions for global convergence of differential evolution algorithm," *J. Appl. Math.*, vol. 2013, pp. 1–14, Aug. 2013.

[61] A. Kumar, B. K. Jha, D. Singh, and R. K. Misra, "Current injection-based Newton–Raphson power-flow algorithm for droop-based islanded microgrids," *IET Gener., Transmiss. Distrib.*, vol. 13, no. 23, pp. 5271–5283, Dec. 2019.

[62] F. Katiraei and M. R. Iravani, "Power management strategies for a micro-grid with multiple distributed generation units," *IEEE Trans. Power Syst.*, vol. 21, no. 4, pp. 1821–1831, Nov. 2006.

[63] M. Marei, E. El-Saadany, and M. Salama, "Flexible distributed generation: (FDG)," in *Proc. IEEE Power Eng. Soc. Summer Meeting*, vol. 1, Jul. 2002, pp. 49–53.

[64] G. Wu, R. Mallipeddi, and P. N. Suganthan, "Problem definitions and evaluation criteria for the CEC 2017 competition on constrained real-parameter optimization," Nat. Univ. Defense Technol., Changsha, China, PR China Kyungpook Nat. Univ., Daegu, South Korea, Nanyang Technol. Univ., Singapore, Tech. Rep., 2017.

[65] M. Hellwig and H.-G. Beyer, "A matrix adaptation evolution strategy for constrained real-parameter optimization," in *Proc. IEEE Congr. Evol. Comput. (CEC)*, Jul. 2018, pp. 1–8.

[66] Z. Fan, Y. Fang, W. Li, Y. Yuan, Z. Wang, and X. Bian, "LSHADE44 with an improved constraint-handling method for solving constrained single-objective optimization problems," in *Proc. IEEE Congr. Evol. Comput. (CEC)*, Jul. 2018, pp. 1–8.

[67] Y. Wang, J.-P. Li, X. Xue, and B.-C. Wang, "Utilizing the correlation between constraints and objective function for constrained evolutionary optimization," *IEEE Trans. Evol. Comput.*, vol. 24, no. 1, pp. 29–43, Feb. 2020.

[68] B.-C. Wang, H.-X. Li, Q. Zhang, and Y. Wang, "Decomposition-based multiobjective optimization for constrained evolutionary optimization," *IEEE Trans. Syst., Man, Cybern., Syst.*, vol. 51, no. 1, pp. 574–587, Jan. 2021.

[69] G. V. Raju and P. Bijwe, "Reactive power/voltage control in distribution systems under uncertain environment," *IET Gener., Transmiss. Distrib.*, vol. 2, no. 5, pp. 752–763, 2008.

BABLESH KUMAR JHA received the B.Sc. degree in engineering from the Muzaffarpur Institute of Technology, Muzaffarpur, in 2006, the M.Tech. degree from the Birsa Institute of Technology, Sindri, Dhanbad, in 2014, and the Ph.D. degree from the Indian Institute of Technology (BHU), Varanasi, India, in 2019. He is currently a Research Associate with the Department of Electrical Engineering, IIT Gandhinagar. His research interests include distribution system operation and planning, demand side management, integration of electric vehicles in distribution system, power system optimization, P2P energy trading, and power flow algorithms.

SWAGATAM DAS is currently working as an Associate Professor with the Electronics and Communication Sciences Unit, Indian Statistical Institute, Kolkata, India. He has 22 500+ Google Scholar citations and an H-index of 70 to date. He has published more than 300 research papers in peer-reviewed journals and international conferences. His research interests include evolutionary computing, pattern recognition, multi-agent systems, and wireless communication. He was a recipient of the 2012 Young Engineer Award from the Indian National Academy of Engineering (INAE) and the 2015 Thomson Reuters Research Excellence India Citation Award as the Highest Cited Researcher from India in the Engineering and Computer Science category, from 2010 to 2014. He is the Founding Co-Editor-in-Chief of *Swarm and Evolutionary Computation*, an international journal from Elsevier. He has also served as or is serving as an Associate Editor for the IEEE TRANSACTIONS ON CYBERNETICS, *Pattern Recognition* (Elsevier), *Neurocomputing* (Elsevier), *Information Sciences* (Elsevier), the IEEE TRANSACTIONS ON SYSTEMS, MAN, AND CYBERNETICS: SYSTEMS, the *IEEE Computational Intelligence Magazine*, IEEE ACCESS, and so on. He is an Editorial Board Member of *Information Fusion* (Elsevier), *Progress in Artificial Intelligence* (Springer), *Applied Soft Computing* (Elsevier), *Engineering Applications of Artificial Intelligence* (Elsevier), and *Artificial Intelligence Review* (Springer).

ABHISHEK KUMAR received the B.Tech. degree in electrical engineering from Uttarakhand Technical University, Dehradun, in 2013, and the Ph.D. degree in systems engineering from the Department of Electrical Engineering, Indian Institute of Technology (BHU), Varanasi, India, in 2019. His developed optimization algorithms EBOwith-CMAR and SASS have secured the first position in IEEE CEC-2017 special session and competition on bound-constrained optimization and IEEE CEC-2020/GECCO-2020 special session and competition on real-world constrained optimization, respectively. His current research interests include swarm and evolutionary computation and its application in real-world optimization problems especially in power system optimization applications and machine learning. He was a recipient of the Young Researcher Award-2016 from the IEEE CIS Chapter, UP section, IIT Kanpur. He also serves as a Reviewer for several journals, including the IEEE TRANSACTIONS ON EVOLUTIONARY COMPUTATION, the IEEE TRANSACTIONS ON CYBERNETICS, *IET GTD*, *SWEVO*, and *ASOC*.

RAMMOHAN MALLIPEDDI (Senior Member, IEEE) received the master's and Ph.D. degrees in computer control and automation from the School of Electrical and Electronics Engineering, Nanyang Technological University, Singapore, in 2007 and 2010, respectively. He is currently an Associate Professor with the Department of Artificial Intelligence, School of Electronics Engineering, Kyungpook National University, Daegu, South Korea. He coauthored articles published the IEEE TRANSACTIONS ON EVOLUTIONARY COMPUTATION, and so on. His research interests include evolutionary computing, artificial intelligence, image processing, digital signal processing, robotics, and control engineering. He also serves as an Associate Editor for *Swarm and Evolutionary Computation*, an international journal from Elsevier and a Regular Reviewer for journals, including the IEEE TRANSACTIONS ON EVOLUTIONARY COMPUTATION and the IEEE TRANSACTIONS ON CYBERNETICS.

• • •